Review

Electrocatalytic reduction of nitrate: Fundamentals to full-scale water treatment applications

Sergi Garcia-Segura[a,*], Mariana Lanzarini-Lopes[a], Kiril Hristovski[b], Paul Westerhoff[a,*]

[a] Nanosystems Engineering Research Center for Nanotechnology-Enabled Water Treatment, School of Sustainable Engineering and the Built Environment, Arizona State University, Tempe, AZ 85287-3005, USA
[b] Nanosystems Engineering Research Center for Nanotechnology-Enabled Water Treatment, The Polytechnic School, Arizona State University, Mesa, Arizona 85212-2880, USA

ABSTRACT

Nitrate contamination in surface and ground waters is one of this century's major engineering challenges due to negative environmental impacts and the risk to human health in drinking water. Electrochemical reduction is a promising water treatment technology to manage nitrate in drinking water. This critical review describes the fundamental principles necessary to understand electrochemical reduction technologies and how to apply them. The focus is on electrochemical nitrate reduction mechanisms and pathways that form undesirable products (nitrite, ammonium) or the more desirable product (dinitrogen). Factors influencing the conversion rates and selectivity of electrochemical nitrate reduction, such as electrode material and operating parameters, are also described. Finally, the applicability for treating drinking water matrices using electrochemical processes is analyzed, including existing implementation of commercial treatment systems. Overall, this critical review contributes to the understanding of the potential applications and constraints of electrochemical reduction to manage nitrate in drinking waters and highlights directions for future research required for implementation.

1. Environmental and health impacts of nitrogen oxyanions in water

Nitrogen is critical to all life, but in the wrong form or wrong place is detrimental to life. In water, nitrogen is commonly found as nitrate (NO_3^-), nitrite (NO_2^-) or ammonium ion (NH_4^+), although other transient and low concentration aqueous nitrogen species exist as part of the natural nitrogen cycle. Nitrogen exists in its most reduced oxidation state (-III) in ammonia and most oxidized state in nitrate ($+V$). Ammonia (NH_4^+/NH_3; $pK_a = 9.25$) is relatively easily transformed via biotic and abiotic processes in the environment to nitrite, nitrate or dinitrogen (N_2) [1]. Nitrate is a non-ligand forming oxyanion that exhibits high mobility and is soluble in water. Nitrate naturally occurs in some geological formations and groundwater. However, nitrate pollution in surface and ground waters is due to anthropogenic activities, including fertilizer runoff from agricultural lands, stormwater runoff from urban surfaces and discharge of sewage or treated wastewater [2–4]. As a result of anthropogenic nitrogen fertilizer inputs, nitrate concentrations in surface and ground waters have dramatically increased during the last century [5,6]. Some anthropogenic nitrate originates from salt mines, but most originates from the Haber-Bosch

process that converts atmospheric nitrogen gas to ammonia which is the major source of much of the nitrogen used in industrial manufacturing and agriculture, which then results in nitrate pollution. Because global industrial nitrogen fixation consumes 2–5% of the worlds energy and because of the detrimental effects of nitrates in water, the US National Academy of Engineers identified the imbalance of the natural nitrogen cycle and efficient management of the nitrogen cycle in water as one of the Grand Challenges for the 21st century [7,8].

Nitrate in drinking water can lead to methemoglobinemia, which is caused by nitrite in the human gastro-intestinal tract [9,10]. Nitrite, which is reduced from nitrate by gastro-intestinal microorganisms, oxidizes the hemoglobin's ferrous ions into ferric ions and consequently disables the oxygen transport mechanisms of the red blood cells. The impaired oxygen transport can produce cyanosis, fatigue, shortness of breath, cerebral anoxia and even death. Infants and fetuses are particularly sensitive to methemoglobinemia, which is also known as the "blue baby syndrome". Nitrate in drinking water has also been implicated in deleterious impacts to the human endocrine system [11–14]. To minimize the adverse health impacts of nitrate, the World Health Organization [15] has set a recommended maximum contaminant level (MCL) of 50 mg/l NO_3^- ($\sim$11 mg/l as N-NO_3^-) in drinking water. The

United States Environmental Protection Agency, however, promulgated a lower enforceable MCL of 10 mg/l as N-NO$_3^-$ [16]. Unfortunately, > 40 million people in the United States still do not have access to municipally-treated water, instead relying mostly on private groundwater wells. Even in public water systems, nitrate is among the most commonly reported water quality violations in the USA [17]. As a result, nearly 23 million people may be exposed to water with nitrate concentrations above regulated limits [6]. Nitrate contamination of groundwater is widespread in China and Europe too [18–20]. Thus, there is a need for efficient nitrate removal technologies suitable for large-scale water treatment systems as well as very small point-of-use (POU) treatment systems within homes. A unique feature of most POU systems is the need for chemical-free treatment.

This review critically examines the current research related to electrochemical technologies for transforming and reducing nitrate to different nitrogen species. Because it is innocuous, nitrogen gas (N$_2$) is the desired and targeted end-product when aiming to manage the nitrogen cycle and minimize the impact of anthropogenic nitrogen, although nitrogen recovery in a usable form as fertilizer (e.g., ammonium) may be also feasible. Nitrogen (N$_2$) has a low solubility in water characterized by a Henry's Law constant of K$_H$ = 6.24 × 10^{-4} mol L^{-1} atm^{-1} [21]. Once formed, N$_2$ is preferentially evolved from solution. Ammonia in drinking water causes its own adverse problems including toxicity towards some aquatic organisms in surface waters, increase disinfectants requirement, and/or cause biological nitrification in water distribution systems. Fig. 1 illustrates the rapid increase in electrochemical reduction research since 1990. This review includes three themes covering the breadth of advances over this period. First, the fundamental electrochemical principles and description of electrolytic cells are presented. Second, mechanisms for direct charge transfer and indirect electrochemical processes involved in the reduction of nitrate are critically reviewed. Special emphasis has been given to the influence of electrodic material selection, crystal phases and electrolytes. Third, integration and application of electrochemical technologies into integrated water treatment systems is reviewed. Finally, the review concludes with a roadmap for future research opportunities.

2. Electrochemical reactors for denitrification

Electrochemical reactors for denitrification are electrolytic cells consisting of at least two electrodes. An electrode is a conductor in contact with electrolytes in aqueous solution. The electrode allows the current circulation through the external electrical circuit, and most importantly, the electrode surface serves to exchange electrons with electroactive species in solution. Electroactive species are reactants in solution that engage in redox reactions by direct charge transfer on the electrode's surface. An anode is the electrode where oxidation processes occur, whereas the cathode is associated with reduction of electroactive
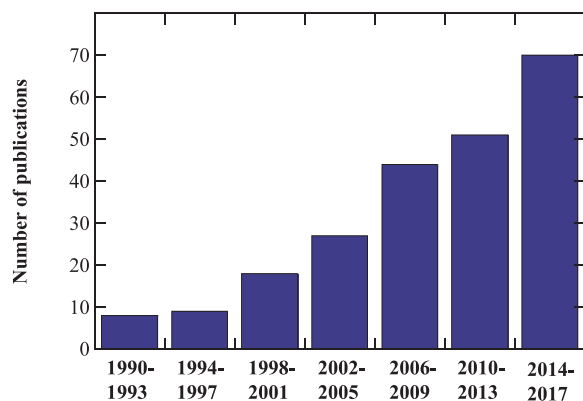
species. In electrochemical denitrification, the objective is complete reduction of nitrate to nitrogen gas. Because nitrate removal involves an electron transfer (i.e., nitrate accepts electrons during the reductive reaction), the focus is on the cathodic reactions. Electrochemical reduction effectiveness is commonly evaluated in terms of current or Faradaic efficiency (FE) from Eq. (1), which determines the number of electrons consumed in an electrochemical reaction relative to the expected theoretical conversion governed by Faraday's law [22].

$$FE \ (\%) = \frac{Q_{exp}}{Q_{theor}} \times 100 = \frac{n \times F \times N_i}{3600 \times I \times t} \times 100 \qquad (1)$$

where Q_{exp} is the experimental charge (Coulomb) consumed in the reaction of interest; Q_{theor} is the total charge (Coulomb) circulated; n is the amount of electrons required per mol of product (mol); F is the Faraday constant (96,487 C mol^{-1}); N_i is the amount (mol) of product generated during the electrolysis; I is the applied electric current (A); t is the time (h); and 3600 is a unit conversion factor (3600 s/h). Reduction and oxidation reactions occur simultaneously at the cathode and anode surfaces in electrolytic cells, respectively. Consequently, when using undivided electrochemical reactors (see Fig. 2a), some reduced species could be re-oxidized on the anode surface, which decreases the overall faradaic efficiency [23,24]. The use of divided cells, however, is considered a suitable alternative that minimizes this undesired effect.

In divided electrolytic cells (Fig. 2b), the anode and cathode are physically separated in two chambers (compartments) commonly referred to as anolyte and catholyte. The two chambers are separated by an ion exchange membrane, or salt bridges, which allow the ions to flow from one half-cell to the other. The ions carrying the charge while preventing the intermixing of solutions between the chambers [25]. For example, when using a cationic exchange membrane (CEM), transporting nitrite (reduced product of nitrate) to the anolyte could be prevented, thereby avoiding its re-oxidation and consequently increasing the faradaic efficiency associated with its production [26]. Divided electrochemical cells have higher ohmic resistance when compared with undivided electrochemical cells under identical conditions, which increases the final energy consumption. Eq. (2) is an example for assessing energy consumption and is critical when optimizing electrolytic cell design:

$$EC = \frac{E_{cell}It}{V_S} \qquad (2)$$

where EC is electrical energy consumption in (kW h m^{-3}); E_{cell} is the cell's electrochemical potential (V); I is the electric current (A); t the reaction time (h); and V_s is the volume of solution treated (m^3). In continuous flow reactor systems, the hydraulic residence time or "reaction" time is computed as V_s divided by flowrate (Q, m^{3}h^{-1}). However, most research is based on batch reactor experiments without flow, so operational time is the duration of the experiment.

Another useful engineering parameter that helps to determine operational costs of energy-dependent water treatment systems is the electrical energy per order (E_{EO}). The E_{EO} quantifies the required electric energy to reduce pollutant concentration by one order of magnitude in a unit volume (kW h m^{-3} order^{-1}) calculated from Eqs. (3) or (4) for batch operation mode or continuous flow mode [27,28], respectively.

$$E_{EO} = \frac{E_{cell}It}{V_S \log(c_i/c_f)} \text{for batch reactors} \qquad (3)$$

$$E_{EO} = \frac{E_{cell}I}{Q_v \log(c_i/c_f)} \text{for flow-through reactors} \qquad (4)$$

where Q_v is the treated water flowrate in (m^{3}h^{-1}); and c_i and c_f are the initial and final pollutant concentrations (mol L^{-1}), respectively. Unfortunately, this parameter has not been commonly reported for nitrate electrochemical reduction treatment although E_{EO} serves as a valuable
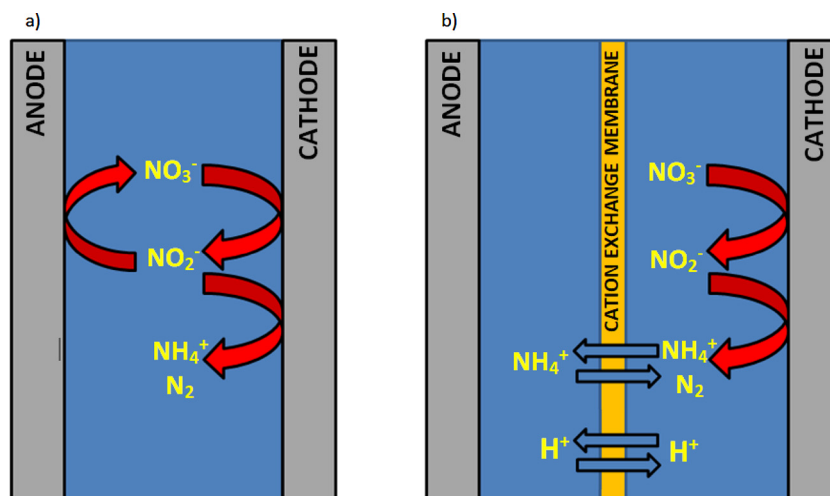

Fig. 1. Number of publications from 1990 until February 2017 on nitrate electrochemical reduction.

Fig. 2. Scheme of (a) undivided and (b) divided electrochemical reactors used in electrochemical reduction of nitrate.

tool to compare many different treatment systems, and not only electrocatalytic systems [27].

Electrolysis involves two different operation modes: potentiostatic and galvanostatic. Potentiostatic electrolysis is conducted by imposing a fixed and constant electric potential (E in V) by an external power supply. Potentiostatic conditions allow better control of nitrate reduction selectivity because only those redox reactions that are thermodynamically possible at a given E may occur. To control the electrode potential, however, a three-electrode system is required: a working electrode, a counter electrode and a reference electrode. The experimental set-up of potentiostatic cells using three electrodes is similar to the electrochemical cells usually reported in fundamental studies by cyclic voltammetry (CV) analysis. However, instead of analyzing current response during a potential sweep, the reference electrode is used to maintain a constant E [22]. For electrochemical nitrate reduction, the working electrode is the cathode where the desired electrochemical reactions occur. Together with the working electrode, the counter electrode completes the electrical circuit. In contrast, the reference electrode is a half-cell with known reduction potential and solely acts as a reference to measure and control the working electrode potential and maintain potentiostatic conditions. Measured potentials are usually referred to the standard hydrogen electrode or SHE ($E^o = 0$ V for $a_{H+} = 1$), although they are usually measured as Ag/AgCl with saturated KCl ($E^o = + 0.197$ V vs SHE) electrodes or saturated calomel electrodes (SCE) $Cl^-/Hg_2Cl_{2(s)}/Hg_{(l)}/Pt$ ($E^o = + 0.241$ V vs SHE). In potentiostatic electrochemical reduction, as well as in CV studies, nitrate reduction usually occurs only when overpotential is present. Overpotential is the potential beyond the theoretically required potential needed for the reduction half-reaction to thermodynamically occur [29]. In the case of nitrate reduction, overpotential stems from the high activation energy [30–32]. The high activation energy typically leads to slower nitrate reduction when compared with

galvanostatic electrolysis. The need for reference electrodes complicates the scalability of potentiostatic systems for long term electrolysis and adds to the complexity of the electrolytic reactor, which hinders cost-effective commercialization.

Galvanostatic electrolysis is conducted by applying a constant current density (j in mA cm^{-2}), which is the ratio of the electrical current (I) circulated through the electroactive surface area of the electrode (A). The current density determines electrokinetics of the system, which is defined by the number of electrons circulated through the electrochemical cell over a period of operational time. In contrast to the potentiostatic systems, the electrochemical cell of galvanostatic systems requires only two electrodes, which allows for easier scalability and industrial applications. However, in absence of potential control, the galvanostatic conditions can enhance competitive reactions, which in turn can decrease the faradaic efficiency.

The galvanostatic electrochemical cell design is scalable and more likely to be applied in full-scale nitrate reduction electrochemical technologies. Fig. 3 illustrates various reactor designs reported in literature. Due to its simplicity and scalability, the most common design is the conventional parallel plate electrochemical filter press cell (Fig. 3a) [33–35]. The small separation between plate electrodes (anode and cathode) in this design minimizes the solution resistivity and the operational cost. These systems are easy to operate and have small physical footprint. Galvanostatic electrochemical cell units are designed by using one anode and one cathode or several anode-cathode pairs connected in parallel. The use of selective ionic exchange membranes allows designing divided electrochemical filter press cells with anolyte and catholyte compartments [36].

Electrochemical reduction of nitrate is limited by mass transfer at the electrode surface and is discussed in detail later. Enhancing mass transfer is one of the engineering challenges faced in reactors design. Using different turbulence promotors or even fluidized bed inert
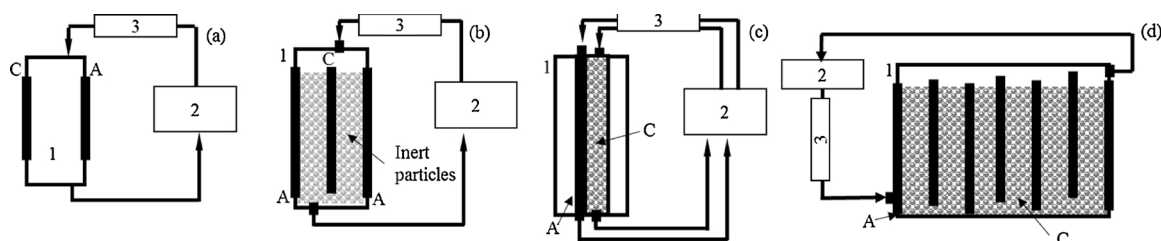

Fig. 3. Electrochemical nitrate reduction reactor set up for (a) plate electrodes cell, (b) fluidizing bed of inert particles cell, (c) packed bed cathode cell and (d) vertical moving particle bed cell. Represented in the figures are the electrochemical cell (1), electrolyte reservoir (2) and flow meter (3). C and A represent the cathode and anode, respectively.
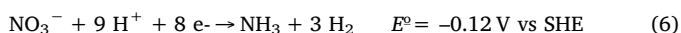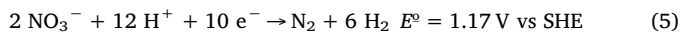
particles in the inter-electrode space have been considered (Fig. 3b) [36]. Moreover, using hydrogenation catalysts as fluidized particles can result in a perfect combination between electrochemical and catalytic processes, where the hydrogen produced as side-reaction on the cathode from water reduction reaction can be employed as reagent for the catalytic reduction [37,38]. Packed bed cathode cells (Fig. 3c and d) are also interesting alternatives to increase cathode electroactive area and mass transfer. These electrochemical cells use packed bed particles or spheres as the cathode. The particles should remain in contact to allow charge circulation, while the solution circulates through them [39].

Even though alternative electrochemical cell designs are feasible, most reactors only incorporate electrochemical filter press cells with plate electrodes (e.g., Fig. 3a). There are tremendous opportunities for further studies and economic analysis to better identify the most competitive design of future commercial electrochemical nitrate reduction units. Improved designs could be based upon computational fluid dynamic models that incorporate molecular diffusion of pollutants to and from the surfaces in addition to improving influent and effluent flow at the reactor ends to improve plug-flow characteristics.

3. Electrochemical nitrogen cycle management

Electrochemistry applications related to various nitrogen forms have been reported for nearly a century. Production of ammonia and sodium hydroxide from electrochemical nitrate reduction was first reported in 1919 [40]. However, after this initial report, most papers focused on developing electroanalytical techniques for quantifying NO_3^- by polarography [41,42], a voltammetric analytic technique that uses dropping mercury electrodes as renewable surfaces in cathodic studies. Nitrate electrochemical reduction for water treatment was reconsidered in the 1980 s as a promising process to recycle caustic solutions of radioactive waste with high nitrate where biological treatments are inapplicable [43–45]. More recently, electrochemical reduction technologies have been applied to treat ion-exchange brines, groundwater, municipal wastewaters and urine [46–49].

The mechanisms for electrochemical conversion of nitrate to nitrogen gas are highly complex, involving numerous reactions, products and stable intermediates (e.g., ammonia, nitrite, hydrazine, hydroxylamine, nitric oxide, nitrous oxide) spanning the many nitrogen oxidation states (from -III up to + V). The Frost-Ebsworth diagram (Fig. 4a) and Pourbaix diagram (Fig. 4b) for nitrogen species illustrate that N_2 and NH_3/NH_4^+ are the thermodynamically most stable forms of nitrogen under standard conditions, especially drinking waters which have pH levels between 6–9. Even though both species would be expected as preferred end products following Reactions (5) and (6), there are several factors such as electrodic material or crystal planes that can alter the final products of electrochemical reduction.

$$2\,NO_3^- + 12\,H^+ + 10\,e^- \rightarrow N_2 + 6\,H_2 \quad E^o = 1.17\,V\ vs\ SHE \tag{5}$$

$$NO_3^- + 9\,H^+ + 8\,e\text{-} \rightarrow NH_3 + 3\,H_2 \quad E^o = -0.12\,V\ vs\ SHE \tag{6}$$

Electrochemical nitrate reduction is usually described in a non-mechanistic way and without intermediates by Reactions (5) and (6). However, several by-products and elementary reactions are needed to describe this complex process. Many variables and operational parameters can affect selectivity and define preferential pathways. Therefore, the mechanistic reduction pathways involving multiple species from several studies were aggregated into a single flow diagram (Fig. 5). The following section summarizes groups of these pathways and identifies knowledge gaps.

3.1. Electrochemical reduction of nitrate to nitrite

As described below, the reduction of nitrate to nitrite is the main barrier (i.e., controls the overall nitrate reduction kinetics) to efficient
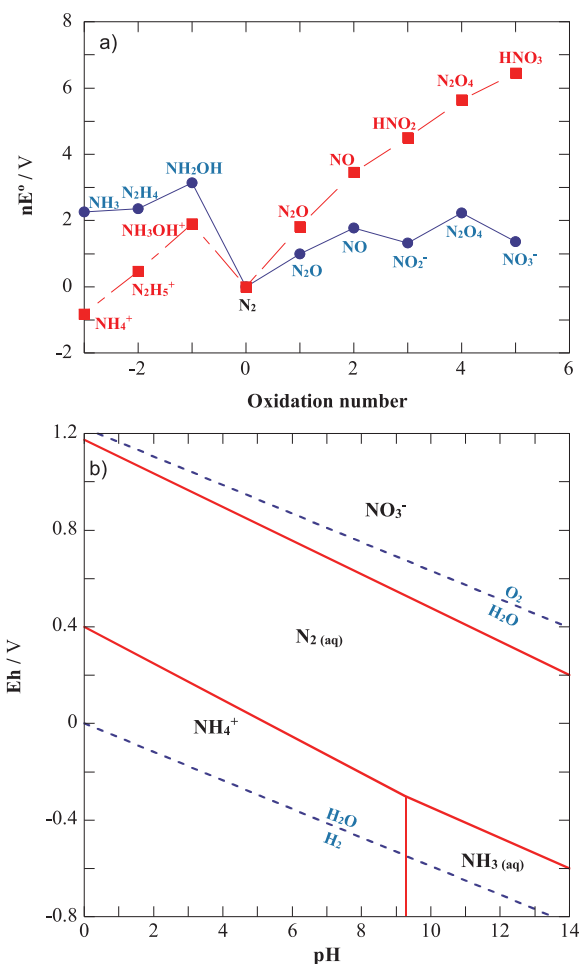

Fig. 4. (a) Frost-Ebsworth diagram of nitrogen species at (■) pH 0.0 and (●) pH 14.0. (b) Pourbaix diagram of nitrogen species.

nitrate removal from water [50]. Improving the understanding of this rate-determining step represents a cornerstone for developing strategies to enhance the charge transfer kinetics and consequently reduce cost and operational times.

The electrochemical reduction of nitrate (Fig. 5) requires an initial adsorption step onto the cathode surface, and co-adsorbing ions from solution inhibit the overall reduction [51,52]. Thus, mass transfer of nitrate from bulk to the electrode surface limits nitrate adsorption, surface-bound nitrate concentrations and consequently overall electrochemical nitrate reduction rate. Electrochemical nitrate reduction is a mass transfer limited process, and consequently the nitrate concentration is relevant because it defines the diffusion rate from solution towards the cathode surface according to Fick's law [31,50,53]. During the treatment of high nitrate concentrations, the amount of free surface catalytic sites on the electrodes determines the achievable reaction rate [54]. Improving surface selectively for nitrate over co-occurring anions and maximizing electrode surface area are critical research needs.

Most papers refer to the formative study by Cunha et al. [31] demonstrating nitrate adsorption and surface bonding on Au electrodes occur through a two-fold coordination acting nitrate as bidentate ligand. The observed two-fold coordination is expected in different metallic anodes, although there are limited reports of similar studies for other electrode materials. The oxygen coordination with the catalytic sites on the electrode surface is highly relevant for activating the transition state that would lead to breaking the N–O bond, which is required for nitrate reduction.

Nitrite is the main quasi-stable intermediate during electrochemical reduction of nitrate before its complete reduction to ammonia or
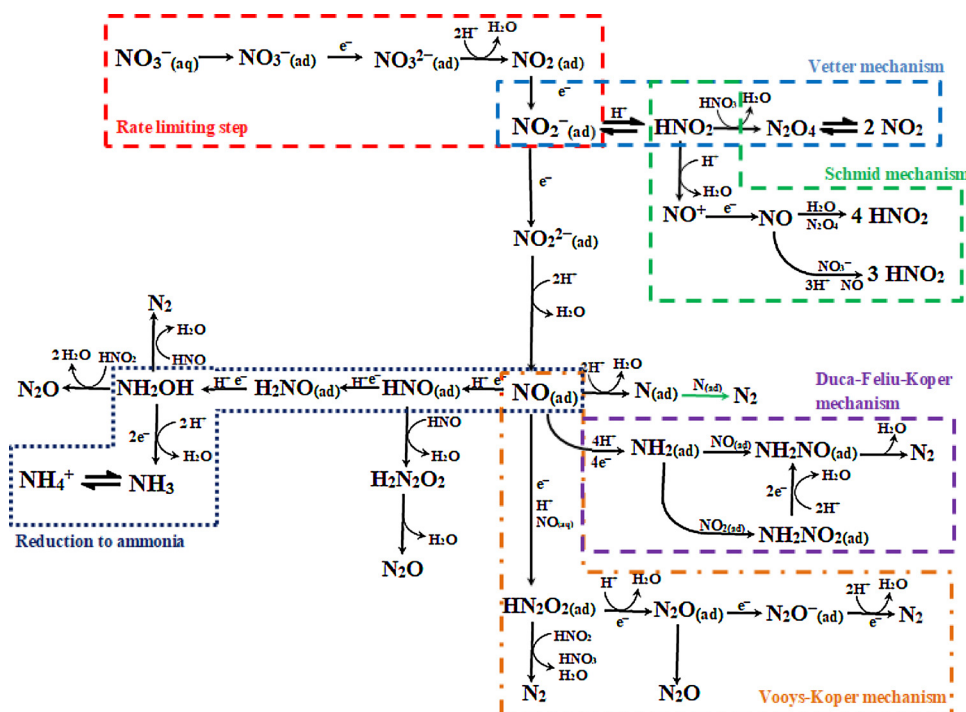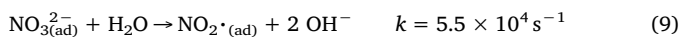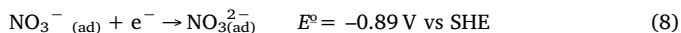
Fig. 5. Mechanisms and main processes during electrochemical reduction of nitrite in water. The overall mechanism is divided into different mechanisms to enhance the understanding and facilitate the description as: Rate limiting step, Vetter mechanism, Schmid mechanism, Duca-Feliu-Koper mechanism, Vooys-Koper mechanism and Reduction to ammonia.

nitrogen gas. Reaction (7) occurs at electrical potentials that are more negative than thermodynamic values, implying that an overpotential is required to initiate the reduction reaction [30–32]. The high activation energy requirement (similar to the one observed for other oxyanions, such as ClO_4^- and SO_4^{2-}) is confirmed by the slow reduction kinetics of nitrate to nitrite.

$$NO_3^- + 2\,H^+ + 2\,e^- \rightarrow NO_2^- + H_2O \qquad E^o = 0.01\ V\ vs\ SHE \qquad (7)$$
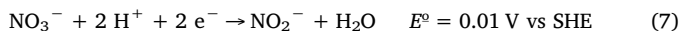
Even though the electrochemical reduction of adsorbed (ad) nitrate to nitrite can be described for the overall Reaction (7), elementary charge transfer reactions of one electron per step result in the formation of adsorbed short-lived intermediates (Fig. 5). The reduction of nitrate to nitrite involves a three-step electrochemical-chemical-electrochemical (ECE) mechanism. ECE mechanisms are defined as a first electron transfer mechanism followed by a homogeneous chemical reaction that yields a more readily reducible species, which is further reduced by a second electron charge transfer. When the chemical reaction is sufficiently fast, a two-electron irreversible process occurs [55]. In the case of nitrate, the initial reduction yields a short lived (~ 20 μs) nitrate di-anion radical (NO_3^{2-}) by Reaction (8) [56,57]. The homogeneous chemical reaction consists of the quick NO_3^{2-} radical hydrolysis and leads to nitrogen dioxide radical ($NO_2\cdot$) according to Reaction (9) [58–60]. Consequently, as illustrated in Reaction (10), $NO_2\cdot$ is further reduced via the second charge transfer reaction pathway to NO_2^-, which may remain adsorbed on the surface [31].

$$NO_3^-{}_{(ad)} + e^- \rightarrow NO_{3(ad)}^{2-} \qquad E^o = -0.89\ V\ vs\ SHE \qquad (8)$$

$$NO_{3(ad)}^{2-} + H_2O \rightarrow NO_2\cdot{}_{(ad)} + 2\,OH^- \qquad k = 5.5 \times 10^4\ s^{-1} \qquad (9)$$

$$NO_2\cdot{}_{(ad)} + e^- \rightarrow NO_2^-{}_{(ad)} + H_2O \qquad E^o = 1.04\ V\ vs\ SHE \qquad (10)$$
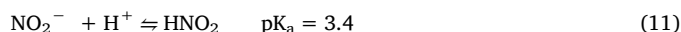
Electrochemical reduction to nitrite, shown by Reactions (8)–(10), is considered the electro-reduction limiting step for the overall reduction mechanism of nitrate to ammonia and nitrogen. The estimated Tafel slopes of 120 mV dec^{-1} support the premise that the first electron transfer is the rate-determining step [51]. Slow electrokinetics, noted by several authors, are attributed to the high energy of the lowest unoccupied molecular π* orbital (LUMO π*) of nitrate, which makes charge injection into the π* orbital highly unfavorable [30–32].

However, because of the similarity in d-orbital energy levels between some metals with highly occupied d-orbitals (Cu, Ag, Pt, etc.) and nitrate's LUMO π*, the unclosed d-orbital shells of the metals have the ability to promote electrochemical reduction of NO3- [61]. Thus, some metals transfer electrons more easily to adsorbed nitrate, making them suitable for applications involving electrochemical nitrate reduction (discussed more below).

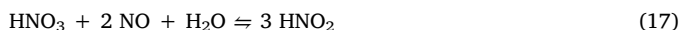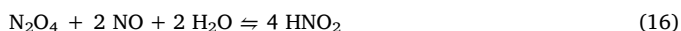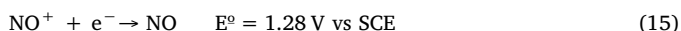### 3.2. Indirect autocatalytic electrochemical nitrate reduction mechanisms

When electrochemical nitrate reduction is carried out at acidic pH and high reactant concentrations (1.0–4.0 M NO_3^-), a secondary pathway for nitrate reduction to nitrite, which simultaneously occurs, may emerge if HNO_2 is present in catalytic concentrations (> 10^{-6} M) [54]. This mechanism is important because it can accelerate the nitrate reduction rates and increase faradaic efficiencies, thus reducing operational costs if strategically used. The autocatalytic reduction of nitrate is considered an indirect reduction mechanism because the nitrate is not the electroactive species, although the overall reaction reduces nitrate to nitrous acid. Reaction rates can rapidly increase if the concentration of the intermediate electroactive species increases, as it is characteristic of autocatalytic reactions. Considering different leading electroactive species in the catalytic cycle results in two possible autocatalytic cycle mechanisms: i) Vetter mechanism [62] or ii) Schmid mechanism [63–65].

The Vetter mechanism involves $NO_2\cdot$ as the electroactive species in the autocatalytic cycle. The electrochemical reduction according to Reaction (10) yields nitrite anion, which then protonates to nitrous acid following an acid-base equilibration under highly acidic conditions (pK$_a$ = 3.4) as described with Reaction (11). The electroactive $NO_2\cdot$ species regenerates following the pathways in Reactions (12) and (13) in which nitrous acid and nitric acid interaction yields dinitrogen tetraoxide (N_2O_4) that quickly disproportionates, releasing two electroactive $NO_2\cdot$ species. In brief, each $NO_2\cdot$ species entering the autocatalytic cycle generates two $NO_2\cdot$.

$$NO_2^- + H^+ \leftrightharpoons HNO_2 \qquad pK_a = 3.4 \qquad (11)$$

$$HNO_2 + HNO_3 \rightarrow N_2O_4 + H_2O \qquad (12)$$

$$N_2O_4 \leftrightharpoons 2\ NO_2\cdot \tag{13}$$

In contrast, the Schmid mechanism involves nitrosonium cation (NO^+) as the electroactive species in the autocatalytic cycle. The NO^+ originates from the protonation of nitrous acid in highly acidic environment according to equilibria summarized with Eq. (14). The electrochemical NO^+ reduction yields nitric oxide (NO) in the bulk as illustrated with Reaction (15) [66]. Two NO species react with N_2O_4 in aqueous media leading to formation of HNO_2 following the pathway described with Reaction (16). This mechanism produces 4 mol s of HNO_2 per 3 mol s of HNO_2 (note that HNO_2 is required to form N_2O_4 according to Reaction (12)). Some authors state the Abel reaction pathway (17) as preferential to Reaction (16) [67,68]. In the Abel reaction pathway, nitric acid directly reacts with the reduced product of the electroactive species (NO) to yield 3 mol s of HNO_2 per 2 mol s of HNO_2 consumed.

$$HNO_2 + H^+ \leftrightharpoons NO^+ + H_2O \tag{14}$$

$$NO^+ + e^- \to NO \qquad E^o = 1.28\ V\ vs\ SCE \tag{15}$$

$$N_2O_4 + 2\ NO + 2\ H_2O \leftrightharpoons 4\ HNO_2 \tag{16}$$

$$HNO_3 + 2\ NO + H_2O \leftrightharpoons 3\ HNO_2 \tag{17}$$

Both mechanisms occur only in highly acidic conditions below nitrate concentrations of 4.0 M where nitric acid naturally decomposes. At nitric acid concentrations > 4.0 M, equilibria (18) and (19) are shifted to the right and lead to the generation of NO and N_2O_4. Even though both NO and N_2O_4 species could lead to HNO_2 formation, this occurs without requiring electrochemical charge transfer reactions. Therefore, these reactions cannot be considered a part of an indirect electrochemical reduction of NO_3^- within an autocatalytic cycle as discussed above.

$$2HNO_3 \leftrightharpoons 2\ NO + 3/2\ O_2 + H_2O \tag{18}$$

$$2HNO_3 \leftrightharpoons N_2O_4 + 1/2\ O_2 + H_2O \tag{19}$$

Some reports provide evidence supporting both mechanisms [69,70]. Koper's group provide experimental evidence that the indirect autocatalytic cycle ends when the reaction of NO with electrogenerated $NO_{(ad)}$ leads to a product not involved in the catalytic cycle [54]. Inhibiting the catalytic cycle due to the consumption of NO agrees with the Schmid mechanism that considers the participation of NO in the catalytic cycle.
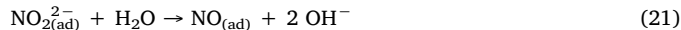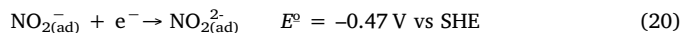
However, the contribution of each of these mechanisms, shown in Fig. 5, remains ill-defined. Dortsiou and Kyriacou [68] observed the autocatalytic cycle at alkaline conditions using a bicarbonate-carbonate buffer. These conditions are more similar to groundwaters used for drinking water supplies, rather than highly acidic pH conditions required for Reactions (14)–(19) to proceed. In this context, it becomes imperative to identify the importance of these autocatalytic cycles at pH ranging from 5 to 10. The further understanding and elucidation of the electrochemical autocatalytic nitrate reduction at pH typical in drinking waters would contribute to design strategies that achieve faster conversion when scaling-up.

3.3. Reduction of nitrite: NO as divergent center towards N_2O, N_2, and NH_3

Nitrite is the first stable intermediate produced during nitrate reduction. However, further electrochemical reduction can yield both undesirable (e.g., NH_4^+) or the desired and innocuous (i.e., N_2) products. Fig. 5 illustrates where adsorbed nitric oxide ($NO_{(ad)}$) may control the electrocatalytic selectivity towards either N_2 or NH_4^+.

The electrochemical reduction of NO_2^- by direct charge transfer Reaction (20) leads to the formation of the dianion radical NO_2^{2-} [71,72]. Similar to the unstable NO_3^{2-}, the dianion radical, NO_2^{2-} quickly hydrolyzes ($k = 1.0 \times 10^5\ s^{-1}$) and produces adsorbed $NO_{(ad)}$
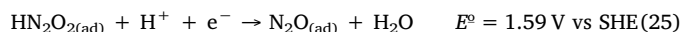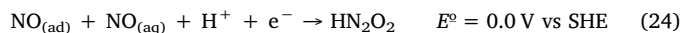
from Reaction (21) [73,74]. The literature lacks information of the role of HONO for these reactions, which exists at low pH.

$$NO_{2(ad)}^- + e^- \to NO_{2(ad)}^{2-} \qquad E^o = -0.47\ V\ vs\ SHE \tag{20}$$

$$NO_{2(ad)}^{2-} + H_2O \to NO_{(ad)} + 2\ OH^- \tag{21}$$

Formation of $NO_{(ad)}$ is central for selective by-product formation. One of the most general N_2 evolution mechanisms considers the reduction of $NO_{(ad)}$ to adsorbed atomic nitrogen ($N_{(ad)}$) according to Reaction (22). Consequently, the adsorbed nitrogen should then react with a second nitrogen atom to form the triple bond of nitrogen following general expression (23) [75]. Unfortunately, this suggested mechanism is not supported by observed experimental results.

$$NO_{(ad)} + 2\ H^+ + 2\ e^- \to N_{(ad)} + H_2O \qquad E^o\ is\ unavailable \tag{22}$$

$$N_{(ad)} + N_{(ad)} \to N_2 \tag{23}$$
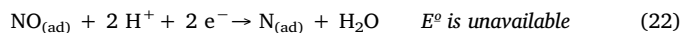
In contrast, the Vooys-Koper mechanism—which is experimentally based on differential electrochemical mass spectroscopy (DEMS) conducted during NO electrochemical reduction kinetic experiments—follows the mechanism described with Reactions (24) and (25) [76,77]. The Vooys-Koper mechanism considers an initial elementary electrochemical reaction involving adsorbed and dissolved NO that forms diazeniumdiolate (HN_2O_2) as a suggested short-lived by-product from Reaction (24) [76,77]. This is facilitated through an Eley-Rideal type reaction, where a solvated species in aqueous solution reacts with a surface-bound NO [74]. This by-product is then easily reduced by a second charge transfer to yield N_2O as summarized with Reaction (25) [54]. The NO dimer as a precursor is one of the most relevant features of this mechanism because the species only forms when $NO_{(aq)}$ is present in solution. Therefore, the reaction with $NO_{(aq)}$ inhibits the Schmid mechanism of the autocatalytic cycle as presented in Eqs. (14)–(17) [54].

$$NO_{(ad)} + NO_{(aq)} + H^+ + e^- \to HN_2O_2 \qquad E^o = 0.0\ V\ vs\ SHE \tag{24}$$

$$HN_2O_{2(ad)} + H^+ + e^- \to N_2O_{(ad)} + H_2O \qquad E^o = 1.59\ V\ vs\ SHE \tag{25}$$

The Chumanov group concluded that the formed N_2O can be further reduced to N_2O^- via Reaction (26) [71], where the electrochemical reduction of such species results in evolution of N_2 following Reaction (27) [78–80].

$$N_2O + e^- \to N_2O\text{-} \qquad E^o = 1.77\ V\ vs\ SHE \tag{26}$$

$$N_2O^- + 2\ H^+ + e\text{-} \to N_2 + H_2O \tag{27}$$
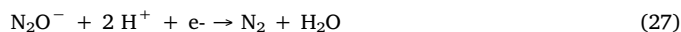
Because the complete reduction of N_2O to N_2 can be made more difficult by the rapid desorption of N_2O, it is important to identify N_2O as a main gas species by DEMS [71,78,81]. Because of the high solubility of N_2O in water ($K_H = 25\ mmol\ L^{-1}\ atm^{-1}$ at 15 °C) [82], solubilized N_2O would be susceptible to be reduced after re-adsorption [54]. Note that the N_2O reduction reaction could become more relevant in long-term electrolysis at large scale than expected from fundamental voltammetric studies.

One of the greatest achievements related to nitrite electrochemical reduction mechanisms is the understanding of the Duca-Feliu-Koper mechanism that demonstrates an alternative and highly feasible N_2 formation deduced from the selective catalytic reduction at quasi-perfect Pt(100) domains [83,84]. A universal room-temperature pathway from nitrite reduction to N_2, similar to the "anammox" bacterial treatment [85], is compelling and important. This pathway (i.e., Duca-Feliu-Koper mechanism) involves the coexistence of $NO_{(ad)}$ and fragments of NH_x species (where x = 0,1,2) stabilized by adsorption on the electrode surface (e.g., Pt(100)). Experimental results reported by Koper's group demonstrate an intermediate region of electric potential ranges where both species are stable (see Fig. 6). This suggest a possible interconversion between NO and NH_x. Indeed, NO generates stable $NH_{2(ad)}$ during reductive stripping as follows (28):
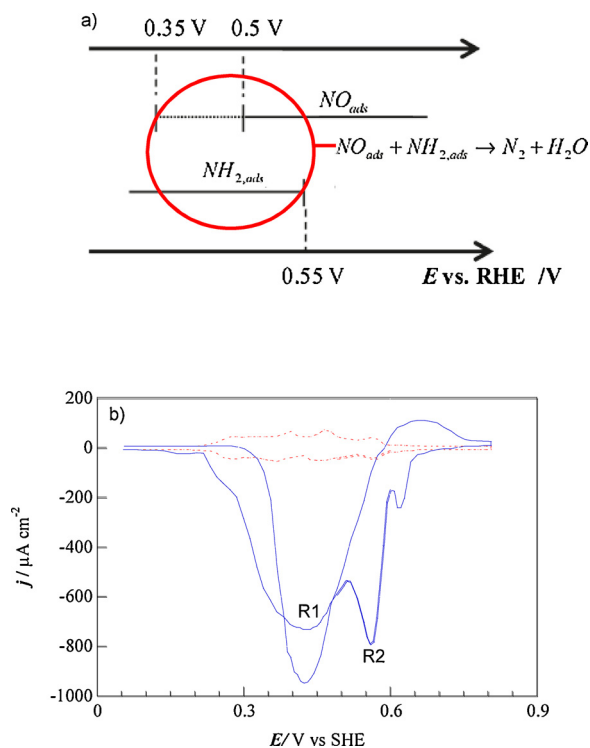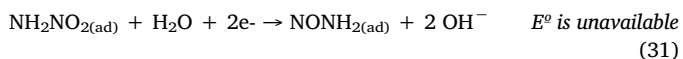
Fig. 6. (a) Potential stability ranges for NH_2 and NO adsorbed species, where solid lines indicate the stability range and dotted lines indicate the theoretical stability range in absence of nitrite in solution. It is highlighted the potential range of coexistence of both species that allows nitrogen evolution reaction. (b) Cyclic voltammetry for nitrate reduction at Pt(100) surface in 0.1 M NaOH at 50 mV/s scan rate (red dotted line) in absence and (blue solid line) presence of 2.0 mM of $NaNO_2$. Cathodic peak R1 corresponds to the direct reduction of nitrite to ammonia, and cathodic peak R2 is ascribed to selective nitrite reduction towards N_2. (For interpretation of the references to colour in this figure legend, the reader is referred to the web version of this article). Figures adapted from [84].
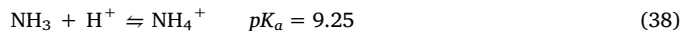
$$NO_{(ad)} + 3\,H_2O + 4e^- \rightarrow NH_{2(ad)} + 4\,OH- \qquad E^o \text{ is unavailable} \quad (28)$$
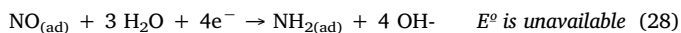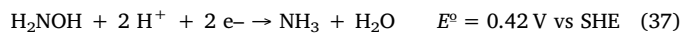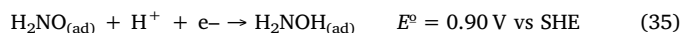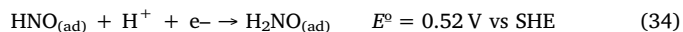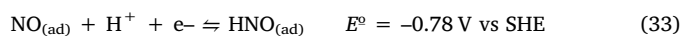
The reduction peak observed at 0.55 V on Pt(100), which is ascribed to the selective reduction of nitrite to N_2 [84], is within the voltage region of coexistence of $NO_{(ad)}$ and $NH_{2(ad)}$ as can be observed in the scheme of Fig. 6. Both species react according to a Langmuir-Hinshelwood recombination Reaction (29) leading to N-nitrosamide ($NONH_2$), which is a transient species that decomposes to generate N_2 according to Reaction (30) [75,86,87].

$$NO_{(ad)} + NH_{2(ad)} \rightarrow NONH_{2(ad)} \qquad (29)$$

$$NONH_{2(ad)} \rightarrow N_2 + H_2O \qquad (30)$$

However, Katsounaros et al. [88] identified nitramide (NH_2NO_2) by gas chromatography-mass spectrometry (GC–MS) and total ion chromatography as a possible intermediate in the N_2 evolution process. Their results suggest that $NONH_2$ would also be produced from the electrochemical reduction of NH_2NO_2 according to Reaction (31). Even though the formation of NH_2NO_2 adduct could be expected from Reaction (32) where NO_2 is the oxo-species involved in reacting with NH_2 [89,90], the formation of such adduct has not been described under electrochemical experiments and still remains unclear. According to the other literature, however, the major product from NH_2NO_2 decomposition is expected to be N_2O [89,90]. This further complicates the understating of this mechanism and necessitates further research.

$$NH_2NO_{2(ad)} + H_2O + 2e- \rightarrow NONH_{2(ad)} + 2\,OH^- \qquad E^o \text{ is unavailable} \quad (31)$$

$$NO_2 + NH_{2(ad)} \rightarrow NH_2NO_{2(ad)} \qquad (32)$$

The last major product yielded during electrochemical nitrite reduction is ammonia (NH_3/NH_4^+). The most accepted mechanism for ammonia formation considers the electrochemical reduction of NO through an electrochemical-electrochemical (EE) mechanism, which has several consecutive direct charge transfer reactions, rather than electrochemical-chemical (EC) mechanism [76]. The reduction of NO leads to the formation of azanone (HNO), also known as nitroxyl, from Reaction (33) [91,92]. The rate determining step is the reduction of HNO to H_2NO according to Reaction (34) [75,76]. This reaction is quickly followed by an additional charge transfer releasing hydroxylamine from Reaction (35) [77], which can be protonated ($pK_a = 5.93$) depending on the pH according to the equilibria (36). Hydroxylamine has been identified and quantified as a by-product of electrochemical reduction [42,93–95], which further supports this mechanism. Ammonia is produced from the fast electrochemical reduction of hydroxylamine [96](37). Ammonia is in equilibrium with ammonium ion (Reaction (38)) [94,97].

$$NO_{(ad)} + H^+ + e- \leftrightharpoons HNO_{(ad)} \qquad E^o = -0.78 \text{ V vs SHE} \quad (33)$$

$$HNO_{(ad)} + H^+ + e- \rightarrow H_2NO_{(ad)} \qquad E^o = 0.52 \text{ V vs SHE} \quad (34)$$

$$H_2NO_{(ad)} + H^+ + e- \rightarrow H_2NOH_{(ad)} \qquad E^o = 0.90 \text{ V vs SHE} \quad (35)$$

$$H_2NOH + H^+ \leftrightharpoons H_3NOH^+ \qquad (36)$$

$$H_2NOH + 2\,H^+ + 2\,e- \rightarrow NH_3 + H_2O \qquad E^o = 0.42 \text{ V vs SHE} \quad (37)$$

$$NH_3 + H^+ \leftrightharpoons NH_4^+ \qquad pK_a = 9.25 \quad (38)$$

The fast reduction of NO to NH_3 could result in low accumulation of hydroxylamine during electrochemical reduction of nitrate at larger scale. However, several chemical reactions may exist that consume H_2NOH and generate N_2 or N_2O following Reactions (39) and (40) [75], respectively.

$$H_2NOH + HNO \rightarrow N_2 + H_2O \qquad (39)$$

$$H_2NOH + HNO_2 \rightarrow N_2O + H_2O \qquad (40)$$

Katsounaros and Kyriacou [75] also identified hyponitrous acid ($H_2N_2O_2$) as a by-product during the electrochemical nitrate reduction. $H_2N_2O_2$ releases from the dimerization of HNO following Reaction (41) and eliminates the possibility of oxyhyponitrite ($H_2N_2O_3$) formation. The release of N_2 from $H_2N_2O_2$ reaction with HNO_2 can be neglected at ambient conditions. Thus, the chemical decomposition (42) of unstable $H_2N_2O_2$ to N_2O is considered [88,98].

$$HNO + HNO \rightarrow H_2N_2O_2 \qquad (41)$$

$$H_2N_2O_2 \rightarrow N_2O + H_2O \qquad (42)$$

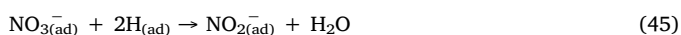### 3.4. Contribution of hydrogenation processes during electrochemical reduction

The adsorption of molecular hydrogen (H_2) can inhibit the electrocatalytic reduction of nitrate as supported via voltammetric analysis [99]. However, NH_4^+ production can be enhanced in the hydrogen adsorption region ($\Delta E < 0.4$ V) despite N_2 formation on platinum (Pt) being a transient process in this ΔE region [100,101]. Thus, hydrogen is not facilitating nitrate reduction to nitrogen by promoting N−N bond formation. Instead, hydrogen promotes N−H bond formation [38]. Nishimura et al. [100] suggested that the termination of N_2O and N_2 evolution in their experiments was probably related not only to the inhibition of NO_3^- adsorption but also to the formation of non-volatile nitrogenized species involving consumption of electrogenerated hydrogen species [100]. This hypothesis could be further supported by the similarities of electrochemical reduction with the catalytic

hydrogenation of nitrate where metallic surfaces are used as catalytic centers for nitrate reduction [102,103].

During electrochemical reduction of nitrate in aqueous media, water is reduced to stable adsorbed elemental hydrogen ($H_{(ad)}$) according to Reaction (43), which is adsorbed on certain metallic surfaces such Pt. Then, H_2 is then generated from the recombination of $H_{(ad)}$ following Reaction (44) with an overall E^o = -0.83 V vs SHE [104].

$$H_2O + e- \rightarrow H_{(ad)} + OH^- \tag{43}$$

$$H_{(ad)} + H_{(ad)} \rightarrow H_2 \tag{44}$$

The contribution of hydrogenation mechanisms to nitrate reduction cannot be directly disregarded because of the strong reducing environment created by the presence of $H_{(ad)}$ with an $E°(H^+/H·)$ = −2.31 V vs SHE [104–106]. Thus, nitrogen intermediate species NO_2^- and NO likely react with $H_{(ad)}$ within the hydrogen evolution reaction region (Fig. 4b), where $H_{(ad)}$ gives rise to NH-adsorbed species. Therefore, these consecutive reactions potentially lead to NH_4^+ by stepwise H_2 addition [107]:

$$NO_{3(ad)}^- + 2H_{(ad)} \rightarrow NO_{2(ad)}^- + H_2O \tag{45}$$

$$NO_{2(ad)}^- + H_{(ad)} \rightarrow NO_{(ad)} + OH^- \tag{46}$$

$$NO_{(ad)} + 2H_{(ad)} \rightarrow N_{(ad)} + H_2O \tag{47}$$

$$N_{(ad)} + H_{(ad)} \rightarrow NH_{(ad)} \tag{48}$$

$$NH_{(ad)} + H_{(ad)} \rightarrow NH_{2\ (ad)} \tag{49}$$

$$NH_{2\ (ad)} + H_{(ad)} \rightarrow NH_{3\ (ad)} \tag{50}$$

Some experimental evidence suggests that a mechanism exists involving the electrocatalytic hydrogenation of adsorbed NO_3^- anion by $H_{(ad)}$ [108–110], where Pt centers would supply the hydrogen atoms required for hydrogenation, similar to what happens with bimetallic catalysts [103,111,112]. The contribution of hydrogenation was also observed during the reduction of nitrate anions using a membrane palladium (Pd) electrode [113]. The reduction rate achieved was substantially higher when hydrogen was supplied from the membrane side opposite to the reaction zone. This phenomenon proves the reduction of N-species chemisorbed on the electrode surface by adsorbed and diffused hydrogen through the Pd membrane electrode.

Katsounaros and Kyriacou [75] suggested the contribution of electrochemical hydrogenation from the balance between the theoretical and quantified evolution of H_2 during the electrochemical reduction of 1 M of $NaNO_3$. As illustrated in Fig. 7, H_2 evolution was not detected in the outgoing gas stream until 105 min, which, according to the authors, can be explained assuming that the reduction takes place through electrochemical hydrogenation. In other words, produced hydrogen is consumed by the high concentration of nitrate in solution inhibiting its evolution by Reaction (44). This observation is supported by the instantaneous detection of H_2 under low concentration of nitrate (0.1 M). If all the electrochemical reductive capacity was consumed in H_2 production (Reactions (43) and (44)) and that nitrate reduction occurs solely due to hydrogenation reactions (Reactions (45)–(50)), then a theoretical amount of H_2 can be estimated per mol nitrate removed. Fig. 7 compares this theoretical amount against the experimental evolution of H_2 and demonstrates that both trends are qualitatively similar, which leads to the conclusion that produced H_2 participates in the reaction mechanism [75]. However, inhibiting hydrogen evolution can be also justified by the competitive electrochemical reduction of nitrate that would consume the circulated charge, diminishing the faradaic efficiency of H_2 evolution. More research is needed to clarify hydrogenation contribution when using Pt electrodes to the nitrate electrochemical reduction mechanisms (Fig. 5).
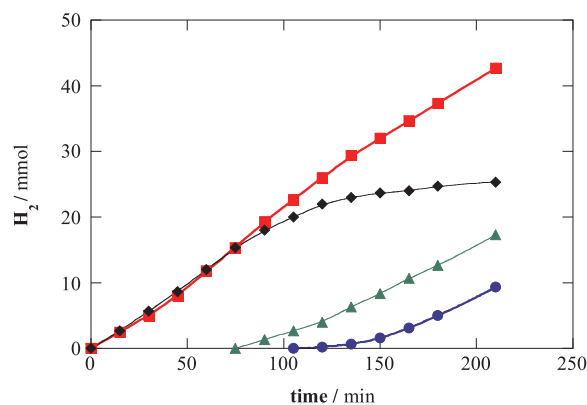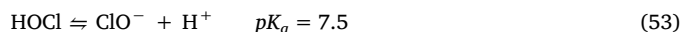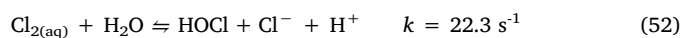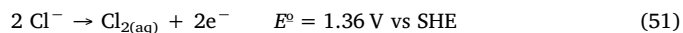

Fig. 7. Evaluation of electrochemical hydrogenation relevance on electrochemical reduction of 1.0 M NO_3^- at −2.8 V vs Ag/AgCl on Sn cathodes: (■) theoretical amount of hydrogen electrogenerated if all the charge passed was consumed for the production of hydrogen; (◆) required amount of hydrogen considering that complete nitrate reduction occurs via electrochemical hydrogenation, (▲) estimated amount of the evolved hydrogen from the difference between theoretical hydrogen evolved and required hydrogen for nitrate reduction, (●) experimental evolution of hydrogen.
Figure adapted from [75].

3.5. Nitrogen gas (N_2) evolution enhancement by simultaneous electrochlorination

The desirable product of nitrate reduction in drinking waters is innocuous N_2 gas, but unfortunately the most commonly reported byproduct in electrochemical treatments is NH_4^+. As previously described, the two compartments of electrolytic cells separate the anode from the cathode. During nitrate reduction, there is a potential to reduce nitrate at the cathode while re-oxidation occurs at the anode. A novel approach has been reported wherein ammonia is scavenged by chlorine before ammonia is re-oxidized to nitrate on the anode. The byproduct of chlorine and ammonia can be N_2, and the process of *in-situ* chlorine production from chloride within the electrolytic cells is termed *electrochlorination*.

Electrochlorination processes consider *in-situ* generation of chlorine active species from the oxidation of chloride ions (Cl^-), an ubiquitous anionic species in drinking water or present at much higher concentrations in ion exchange brines which use 5% to 20% NaCl [114,115]. With proper anode material selection, chloride oxidation and evolution of aqueous chlorine occurs according to Reaction (51) [25,48,116]. Reactions (52) and (53) show the chlorine disproportionation in water [117–120].

$$2\ Cl^- \rightarrow Cl_{2(aq)} + 2e^- \qquad E^o = 1.36\ V\ vs\ SHE \tag{51}$$

$$Cl_{2(aq)} + H_2O \leftrightharpoons HOCl + Cl^- + H^+ \qquad k = 22.3\ s^{-1} \tag{52}$$

$$HOCl \leftrightharpoons ClO^- + H^+ \qquad pK_a = 7.5 \tag{53}$$

Active chlorine species ($HOCl/OCl^-$) are used widely in water reclamation processes to lower ammonia concentrations (i.e., breakpoint chlorination) [121,122]. Chlorination of ammonia generates chloramines following Reactions (54)–(56). Because chloramine species have a moderate oxidizing power and thus react less with dissolved organic matter, they form fewer organochlorinated by-products. As such, chloramines are increasingly used as an alternative to conventional chlorination and serve as microbial disinfectants for nearly half the population of the USA [116,123–128]. Consequently, residual chloramines in drinking water are not a health concern, and in fact may be desirable.

$$NH_3 + HOCl \rightarrow NH_2Cl + H_2O \tag{54}$$

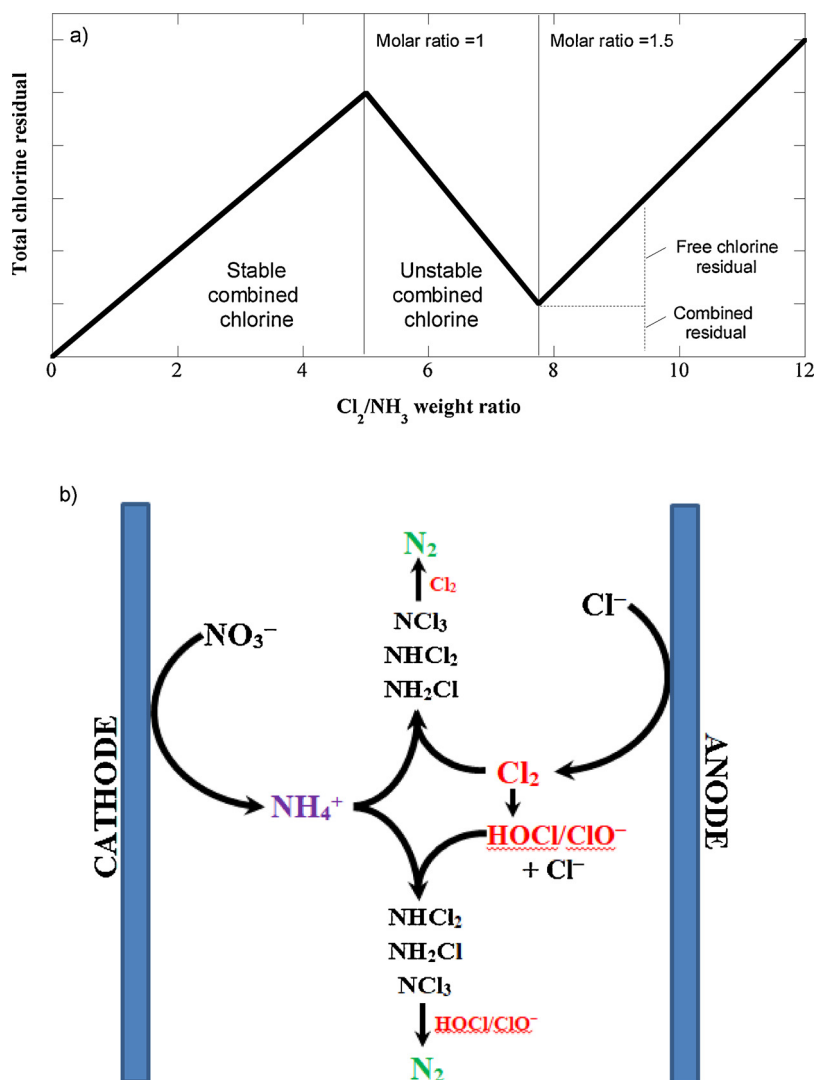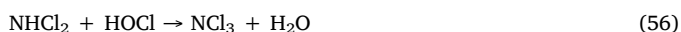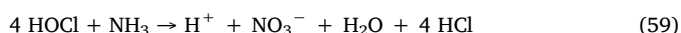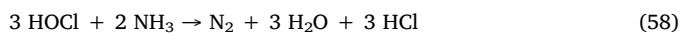$$NH_2Cl + HOCl \rightarrow NHCl_2 + H_2O \tag{55}$$
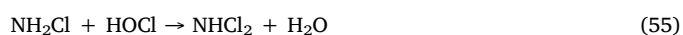
Fig. 8. (a) Formation of combined chlorine (chloramines) represented as total chlorine residual distribution as a function of the Cl_2/NH_3 weight ratio [129]. (b) Scheme of simultaneous electrochlorination mechanism that enhances N_2 production during electrochemical reduction of nitrate.

$$NHCl_2 + HOCl \rightarrow NCl_3 + H_2O \qquad (56)$$

$$NH_2Cl + H_2O \rightarrow HOCl + NH_3 \qquad (57)$$

When the concentration of active chlorine species is greater than a molar ratio of unity with respect to NH_3/NH_4^+ in solution, the nitrogenized species in solution decreases to a minimum residual of chloramines so-called break point (see Fig. 8a) [129]. The decrease is explained by the overall oxidation of chloramine species to nitrogen gas and nitrate ion following Reactions (58) and (59), respectively, even though chloramines conversion to nitrogen at break-point chlorination is the dominant reaction [25,121]. The combined electrochemical process is summarized in Fig. 8b.

$$3\ HOCl + 2\ NH_3 \rightarrow N_2 + 3\ H_2O + 3\ HCl \qquad (58)$$

$$4\ HOCl + NH_3 \rightarrow H^+ + NO_3^- + H_2O + 4\ HCl \qquad (59)$$

Electrochlorination can improve the selectivity towards N_2 evolution (~100%) during electrochemical nitrate reduction [130–133]. In this context, metal oxide anodes are considered because of their suitable electrocatalytic properties for chlorine evolution. However, existing research on electrochemical nitrate reduction neither analyzes the chloramine speciation nor residual chloramine concentrations exiting the electrolytic cell. The generation of concentrated chloramine

effluents could be an added value of the electrochemical reduction process, which in one step would: (i) reduce the content of nitrate in water by transformative technologies with non-added chemicals and (ii) produce *in situ* disinfectant species required in drinking water applications.

4. Factors influencing performance and selectivity of electrochemical nitrate reduction

Although the working electrode potential defines the thermodynamically feasible processes, there are additional factors that influence the selectivity of this electrochemical transformative technology and determine which of four main stable products (NO_2^-, NH_3/NH_4^+, N_2O or N_2) dominates.

4.1. Cathode material selection influence on transformation rates and product speciation during nitrate electrochemical reduction

4.1.1. Selectivity and electrocatalytic response of pure metals electrodes

Early electrochemical work with nitrate was related to using polarography as an electroanalytical tool, rather than a drinking water treatment system, where mercury (Hg) was employed as a pure metal electrode [41,42]. Although hazardous mercury is toxic and prohibitive

Fig. 9. Metallic elements used as cathodic materials for electrochemical reduction of nitrate.
Periodic table adapted from [218].

for uses in water treatment applications, studies using mercury electrodes helped provide fundamental understanding for the role of d-orbital electrons in promoting charge injection in the lowest unoccupied molecular π^* orbital of nitrate [61]. These studies also paved the way for using electrodes made of noble metals (Cu, Ag, Au) and platinoids (Ru, Rh, Ir, Pd and Pt), which also have highly occupied d-orbitals and unclosed d-orbital shells. These similar structures result in their presence in similar groups of the periodic table (Fig. 9).

4.1.1.1. Noble metals as highly electrocatalytic cathodes. Noble metals are excellent materials because of their electrocatalytic properties and stability. Fig. 10 depicts comparative cyclic voltammograms of several noble metals in absence (blank) and presence of NO_3^-. Higher current densities at the reduction potentials range indicate a higher electrokinetics and consequently a faster reduction of NO_3^- on the electrode surface. Thus, as evident from the voltammetric analysis of nitrate reduction shown in Fig. 10 [51], the electrocatalytic properties of noble metals decrease in the order Cu > Ag > Au. Considering the higher electrocatalytic properties of copper, it is not surprising that this

metal has been widely researched; the use of gold and silver electrodes has also been studied [24,59,105,134].

Copper exhibits the highest electrocatalytic reduction kinetics of nitrate to nitrite, which is the rate limiting step of the overall nitrate reduction process to nitrogen or ammonia [51,73,135]. This faster reduction is explained by enhancing the first charge transfer reaction of the adsorption-controlled Reaction (8) for the rate limiting step mechanism described in Fig. 5 [95]. Electrochemical reduction of NO_3^- on copper electrodes has been reported at pH ranging from acidic to highly alkaline [51,136,137]. In alkaline environments, copper gradually deactivates due to cathode passivation involving the creation of an outer layer of shield material that inhibits the electrocatalytic properties. Bouzek's research group reported a current efficiency decrease from 36.5% to 8.0% after 6 h of continuous electrolysis in alkaline conditions [36]. The electrocatalytic passivation was associated with the formation of amorphous copper powder on the electrodes surface due to the decomposition of copper hydrides (CuH, CuH_2) produced at highly cathodic potentials [36,138]. An alternative to employing copper cathodes is to conduct treatment in presence of aqueous Cu ion. Cu ions

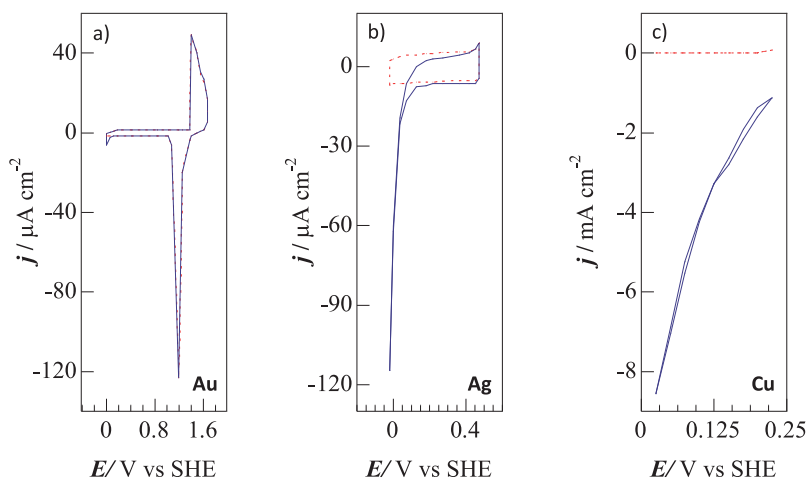**Fig. 10.** (a) Gold, (b) silver and (c) copper cyclic voltammograms recorded at scan rate 20 mV s^{-1} in 0.5 M H_2SO_4 (dashed red line) and 0.5 M H_2SO_4 in presence of 0.1 M $NaNO_3$ (solid blue line). (For interpretation of the references to colour in this figure legend, the reader is referred to the web version of this article).
Figure adapted from [51].

prevent decreases in catalytic activity because Cu deposition forms new active sites on the cathode surface [36]. Avoiding passivation and maximizing catalytic performance of copper electrodes can also be achieved by periodic potential reversal technique, where the electrode acts intermittently as anode and cathode, and the electrocatalytic activity is achieved by continuous refreshment of Cu surface [139].

In contrast, copper passivation has not been reported in acidic media because of the dissolution of copper. Copper spontaneously dissolves under open-circuit conditions in acidic nitrate solution [51]. The continuous dissolution and re-deposition of Cu regenerates the Cu surface and prevents electrode poisoning and passivation.

Copper surface regeneration does not depend on pH when single-cell electrolysis is being performed in presence of chloride [114,131]. In such scenarios, copper dissolution and formation of adsorbed CuCl are facilitated by chlorine active species induced corrosion. This process forms a more porous and rougher electrode surface and consequently creates a higher electrical current density for electrochemical nitrate reduction [140].

Copper can induce rapid nitrite formation kinetics. However, prolonged electrolysis can convert nitrite to ammonia as the main undesirable by-product [34,141]. Unfortunately, few studies demonstrate evolution of N_2 gas [34], except when this process is combined with electrochlorination [131]. However, fundamental studies have been reported that characterize evolution of other nitrogen volatile species via differential electrochemical mass spectroscopy. For example, Dima et al. [51] observed increases in NO production with reduction in current density, without identifying any N_2O. This can be explained by the lower energy of NO sorption on copper surfaces ($\sim 100\,kJ\,mol^{-1}$) when compared to other metal surfaces such as Pt, Pd, Ru, and other plationoids ($\sim 200\,kJ\,mol^{-1}$). Lower sorption energy favors faster desorption, which hinders further reduction of NO. Although desorbed, NO remains in solution because of its high solubility in water ($K_H = 1.94\,mmol\,L^{-1}\,atm^{-1}$ at 20 °C) [142]. Prolonged NO generation reduces desorption rates and causes it to be further reduced to ammonia during long electrolysis [34,141].

The use of Ag electrodes denoted clear nitrate reduction peaks prior to water reduction, whereas the complete reduction to ammonia takes place in the hydrogen evolution reaction region [59]. Effective reduction of nitrate to nitrite and ammonia was also observed on gold electrodes [105,143]. During the galvanostatic electrolysis of 0.5 M $NaNO_3$ at pH 12.5 at 2.85 mA cm^{-2} on bare Au electrodes, nitrite and ammonia yields were estimated at 42% and 58%, respectively, 6 h of treatment [144]. However, both electrodic materials present lower electrocatalytic properties and slower kinetics of nitrate electrochemical reduction.

Long-term use of copper electrodes is prohibitive because of corrosion that compromises electrode stability, along with copper leaching and unwelcome generation of ammonia. However, the high electrocatalytic response highlights copper as one of the most promising electrode materials. In contrast, although silver and gold electrodes may also have good performance, they may be cost prohibitive for drinking water treatment applications (see Table 1). Moreover, ammonia is also identified as main reduction product for silver [59] and gold electrodes [143,144].

4.1.1.2. Platinoids as selective cathodes. Platinum-group metals (PGMs) or platinoids (osmium, ruthenium, iridium, rhodium, platinum, and palladium) are transition metals with great resistance to corrosion and excellent catalytic properties [145,146]. From the cyclic voltammograms of platinoid metals recorded in absence (blank) and presence of NO_3^- (Fig. 11), the electrocatalytic activity for nitrate reduction decreases in the order Rh > Ru > Ir > Pd – Pt [51] as deduced from the decreasing current densities observed under identical experimental conditions. Although osmium is in the plationid metal group, its extreme toxicity prevents it from being used in water treatment applications [147].

Despite their lower electrocatalytic activity, Pt and Pd are the most studied platinoid metals for electrochemical reduction because their electrocatalytic sites are not poisoned by reduction by-products as observed for other platinoids. Poisoning usually occurs due to the strong adsorption of a species on the catalytic sites that prevents the electrode from showing their natural electrocatalytic properties, in this case inhibiting the electrocatalytic reduction of nitrate. Poisoning may stop nitrate reduction in long-term performance. The lower electrocatalytic activity of Pt and Pd is associated with the competitive hydrogen evolution. As seen in the low potential region of the voltammograms that corresponds to the cathodic reduction of nitrate (Fig. 11), nitrate reduction occurs at potentials of high hydrogen coverage (compare to blank voltammogram). This implies that nitrate is unable to competitively adsorb [94] because of the low enthalpy of nitrate sorption on Pt and Pd when compared to hydrogen [51,99].

Platinum and palladium also generate several N-intermediates, which suggests a non-preferred reduction pathway (Fig. 5) on polycrystalline electrodes [148]. Similar to the majority of macroscopic metallic materials, polycristalline electrodes are solid materials composed of many crystallites of different sizes and orientations. Different distribution of preferential species has been observed under potentiostatic conditions [100]. However, strong structure sensitivity is observed when single crystal Pt electrodes with preferential crystal planes are used [50]. Thus, selectivity towards N_2 gas evolution can be maximized.

Even though other platinoids (Ir, Ru, and Rh) show higher electrocatalytic response for nitrate reduction, these cathodic materials are usually not considered for long term applications because their catalytic performance is reduced by the poisoning caused by strong and irreversible adsorption of intermediates (e.g., NO) on the electrode surface [51,148,149]. Poisoning processes can be explained by the Sabatier principle, which states that the interactions between catalyst and substrate should be neither too strong nor too weak. Catalytic sites must bind the adsorbates strong enough to enable activation of reactants. However, the binding strength of the reaction by-products should be weak enough to favor desorption, thus avoiding catalyst poisoning [150,151]. For example, even though Ir electrodes show an onset potential of nitrate reduction at less negative potentials than Pt, a limiting current associated with the surface saturation by adsorbed intermediates poisons the electrode surface and reduces the catalytic performance [149]. Similar behavior is described for Ru electrodes, where the strong adsorption of reactive intermediates has adverse effects on the overall activity [51].

The main limitation for Pt and Pd electrodes is associated with the sluggish kinetics of the first charge transfer reaction. However, the possible selectivity control towards N_2 after surpassing the rate limiting step highlights these metals as promising electrode materials. Although the use of pure platinoid electrode plates is currently cost-prohibitive (see Table 1), using nanoparticles as electrocatalysts emerges as a competitive approach to enhance kinetics by increasing electroactive area and simultaneously reducing material cost.

4.1.1.3. Other metals as electrodic materials. Even though noble and

Table 1
Market cost of pure noble metals and platinoids.

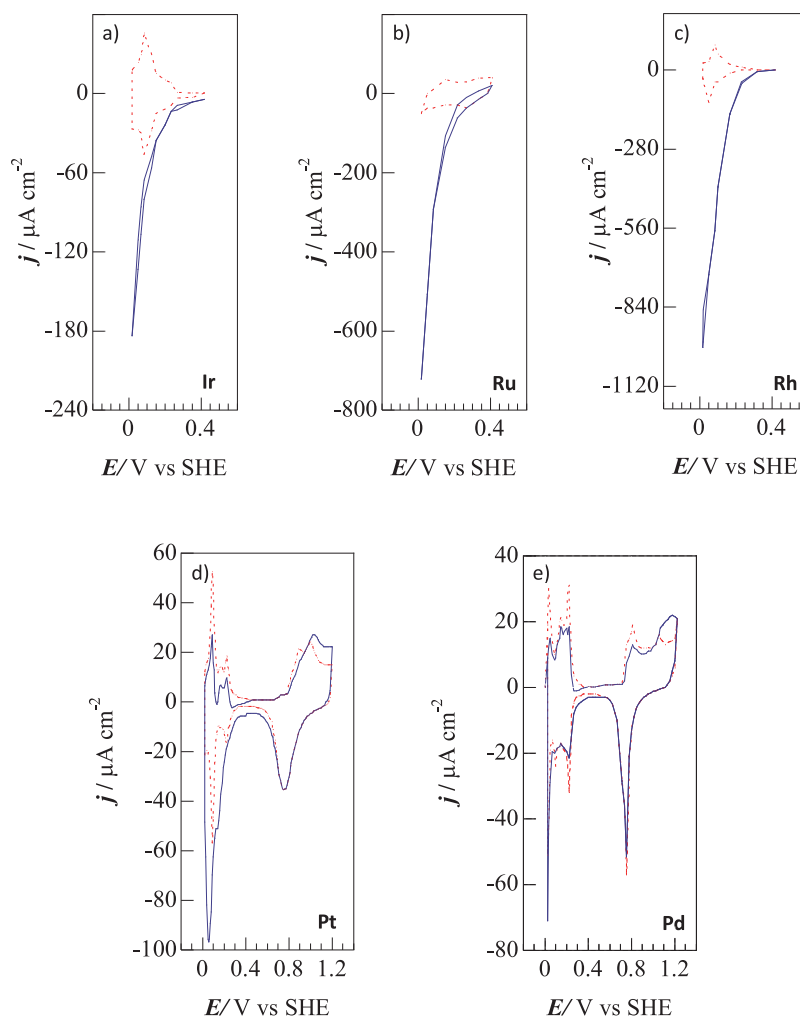| Metal	Symbol	Market Cost ($ kg^{-1})
Copper	Cu	~ 6
Silver	Ag	~ 534
Ruthenium	Ru	~ 2,500
Palladium	Pd	~ 30,000
Platinum	Pt	~ 30,000
Iridium	Ir	~ 34,000
Gold	Au	~ 40,000
Rhodium	Rh	~ 42,000

Fig. 11. (a) Iridium, (b) ruthenium, (c) rhodium, (d) platinum and (e) palladium cyclic voltammograms recorded at scan rate 20 mV s^{-1} in 0.5 M H$_2$SO$_4$ (dashed red line) and 0.5 M H$_2$SO$_4$ in presence of 0.1 M NaNO$_3$ (solid blue line). (For interpretation of the references to colour in this figure legend, the reader is referred to the web version of this article).
Figure adapted from [51]

platinoid metals are among the most researched materials, studies focusing on other metals have also been considered. Low nitrate conversion rates were observed, which classified metallic Ti as a poor catalyst for nitrate reduction. However, when titanium was anodized to form TiO$_2$ nanotubes, it significantly increased the surface area of the electrode, and the nitrate conversion rates improved. The use of titanium nano-cathodes for electrochemical nitrate reduction has been recently proposed by [125], although these electrodes show high selectivity towards ammonia release.

A few studies show that iron exhibits satisfactory performance as an electrode material for nitrate reduction [152]. The high corrosion and dissolution of iron in highly acidic and alkaline pH conditions, commonly employed in reduction of nitrate, represent a significant drawback because these conditions severely compromise the electrode stability, especially over prolonged use. Electrochlorination further compromises the stability of the iron electrodes because Cl$_2$ and HClO/ClO$^-$ induce pitting corrosion effects, which could not be neglected even though iron is considered inexpensive and expendable cathode material [26,152,153]. The main product found when using iron cathodes is ammonia, and small evolution of nitrogen gasses has been also observed.

Nickel with an [Ar] 4 s^2 3d^8 electronic structure has the ability to create an open and closed 3d electron shell allowing for potentiostatic nitrate reduction with selectivity towards N$_2$ of 70% [44]. Nitrate

reduction occurs overlaps H$_2$ evolution at more cathodic potentials and lower current efficiencies than Cu [138,154,155], with discrete current efficiencies of 13%. According to these results, Ni electrodes have lower electrocatalytic activity than Cu for NO$_3^-$ reduction and cannot be considered competitive.

Tin electrodes achieved high selectivity of > 80% towards nitrogen gases, but separate cathode potentials of < –2.9 V (vs Ag/AgCl electrodes) are required to initiate nitrate reduction [75,88,156]. Unfortunately, tin cathodes corrode at potentials of –2.4 V vs Ag/AgCl, which renders this material unstable. Drinking water currently contains tin on the order of 1–10 μg/L [157]. Tin exhibits low toxicity in drinking water and is not currently regulated in the USA or by the World Health Organization. However, the Sn(II) ions resulting from the corrosion act as catalysts [158]. It may be possible to employ tin electrodes in drinking waters, but it will be essential to monitor tin release into the treated water.

Bismuth requires potentials below –2.0 V (vs. Ag/AgCl) to efficiently reduce nitrate [45] and shows lower cathodic corrosion than tin [68]. Bismuth exhibits slower nitrate reduction [45], and exhibits inferior selectivity toward gaseous products (28.2% N$_2$, 14.5% N$_2$O) compared with tin (46.7% N$_2$, 40.7% N$_2$O) [159]. Bismuth has very low toxicity potential in drinking water [160,161], but the continuous leaching of bismuth ions occurs during nitrate electrochemical reduction [45,159] and should be carefully considered as a barrier for its

adoption by regulators.

4.1.2. Metal alloys in the electrocatalytic-selectivity nexus

Alloys are metallic compounds composed by mixing two or more components with at least one of those being a metal. Alloys can be formed by mixing two metals like bronze (Cu and Sn) or a metal with non-metal elements such as steel (Fe and C). An alloy may result in a solid solution (i.e., single phase) or a mixture of differentiated phases. Alloys can present different properties than the individual elements that compose them. The application of binary or ternary alloys as electrodes should lead to (i) higher N_2 selectivity as the final product and (ii) enhanced catalytic activity towards NO_3.

4.1.2.1. Copper alloys to enhance copper selectivity.
Copper alloys (bronzes, brass, and cupronickels) have been studied because of the high electrocatalytic properties shown by pure Cu for electrochemical nitrate reduction. With nitrite and ammonia released as main products using pure copper cathodes, the study of alloys aims to steer the product selectivity towards nitrogen evolution while increasing (or maintaining) the nitrate reduction rates.

Bronzes are alloys mainly composed of Cu and Sn. As discussed above, Sn cathodes present higher N_2 evolution selectivity [88,156], which is the desired outcome for environmental application of electrochemical reduction technologies. Increasing Sn percentage up to 12 wt. % in the alloys results in (i) accelerated reduction rates and (ii) enhanced selectivity towards N_2 at highly cathodic potentials (–1.40 V vs SHE) [23]. However, ammonia remains the preferential product [162]. Higher Sn contents reduce the alloy catalytic properties and thus have a detrimental effect. Alloys with Sn > 49 wt. % have almost identical electrochemical behavior to that of pure Sn, due to similar polarization curve, regardless of Sn content [163]. Mácová et al. [23] suggested that the different electrocatalytic behaviors may be explained by the metallographic structure of these alloys as expected from bronze phase diagrams. Single phase α present up to 15.8 wt. % Sn was identified as the most electrocatalytic phase. The δ phase and the eutectoid mixtures of $\alpha + \delta$ ($Cu_{31}Sn_8$) were associated with a rapid decline in catalytic response. Nevertheless, other structural effects, such as preferred crystallographic planes that could also play an important role, were not considered in this correlation. Even though nitrogen selectivity increases considerably when using bronze cathodes, the possible Sn leaching needs to be analyzed under long-term electrolysis conditions before implementation.

Brasses are alloys similar to bronze but mainly composed of Cu and Zn. Brasses exhibit more electrocatalytic activity than pure Cu. The maximum electrocatalytic response for brass alloys occurs at 41 wt. % of Cu [164] without showing poisoning effects observed on pure copper electrodes [165]. Unfortunately, long-term electrolysis may show significant Zn leaching, thus modifying the alloy composition. For example, Mattarozi et al. [165] reported a composition change from $Cu_{70}Zn_{30}$ to $Cu_{74}Zn_{26}$ after 8 h of electrolysis under $E = -1.4$ V vs Hg/HgO/1 M KOH reference electrode. Note that this side-effect could become more prominent when electrochemical reduction is performed along with the electrochlorination process [114,166,167].

Even though zinc recommended MCL following secondary drinking water standards by EPA are as high as 5.0 mg L^{-1} [168], long-term exposure to high levels of Zn may induce hypocalcaemia and bone resorption [169]. Brasses could reduce electrode material costs, but their poor stability compromises their use for water treatment purposes.

Cupronickels are alloys of Cu that contains Ni and other minor strengthening elements such as iron and manganese. Cupronickels are highly resistant to corrosion in seawater (high chloride content) and as such have been explored as cathodes for nitrate reduction in high saline conditions such as brines. Increasing Ni weight content considerably increases Faradaic efficiencies of ammonia release but decreases the electrochemical reduction kinetics of nitrate [155,170]. Therefore, a direct benefit of these alloys as cathodes for electrochemical reduction of nitrate in drinking water has not been reported. However, cupronickels' corrosion resistance in highly saline media and preferred ammonia generation suggest they may be suitable for applications that employ simultaneous electrochlorination [135].

4.1.2.2. Platinoid alloys to enhance kinetics while maintaining selectivity towards N_2.
The preferred selectivity towards nitrogen evolution of platinoid electrodes drives research towards enhancing their sluggish reduction kinetics. Thus, the use of bimetallic alloys with platinoids as the parent metal appears to be a possible strategy to enhance electrocatalytic response.

Alloys comprised of platinoid metals aim to improve electrocatalytic performance by combining a catalyst-substrate with strong adsorbate interaction and a catalyst-substrate with weaker interaction, as observed in volcano plots explained by Sabatier principle, as discussed previously. Consequently, electroactive species adsorption can be ensured while reducing electrode poisoning. For example, Rh-Pt alloys show less poisoning during cathodic scan than pure Rh electrodes [148]. Furthermore, improved kinetics are observed with Rh/Pt(100) alloys, although they exhibit preferred selectivity towards ammonia formation [171]. Similar trends have been reported with Ir-Pt alloys where the different metals in the alloy act preferentially as adsorption sites or reducing centers [149]. Platinoid-platinoid alloys have not been identified as competitive electrodes because of low performance, low selectivity, or high cost.

Bimetallic alloys with copper combine the great selectivity of pure platinoid electrodes with the quick reduction kinetics observed in pure Cu electrodes. On Cu-Pt(100) alloy electrodes, Cu sites favor quick reduction of nitrate at potentials below 0.2 V, being the NO_2^- yielded adsorbed on the Pt(100) surface. Further reduction towards nitrogen is described by the Duca-Feliu-Koper mechanism (see Fig. 5), which was observed on pristine Pt(100) electrodes [171]. Therefore, the Pt-Cu alloy showed improved performance compared with pure Cu and Pt electrodes [171,172].

On Cu-Pd alloy electrodes, Cu enhances nitrate reduction in the rate determining steps (i.e., initial adsorption and first charge transfer). The linear correlation between activities of electrode with Cu coverage (see Fig. 12) clearly evidences the role of Cu as promoter. Meanwhile, the Pd sites are associated with subsequent reduction towards N_2. However, copper has a negative effect on the selectivity after promoting the initial step, which explains the maximum observed N_2 yield depending on Cu coverage (Fig. 12) [173]. Further analysis of volatile species indicates that low copper covering of Cu on Pd is associated with N_2 evolution, whereas higher Cu content enhances N_2O generation. The evolution of N_2O on Cu-Pd is interesting because pristine Cu surfaces evolve solely NO due to the low sorption of this species, which it hinders its further reduction [51]. These results suggest that NO is adsorbed on Pd catalytic sites and demonstrates the interaction between Cu and Pd [107,173,174].

Principles similar to those underlying the catalytic hydrogenation mechanisms help explain high performance of Cu-Pd alloys as electrodes. Excellent performance has been reported for Cu-Pd bimetallic alloys when applied for catalytic hydrogenation [102,103]. Thus, the study of such materials in electrochemical reduction processes highlights the nexus between transformative technologies for nitrate treatment [57,103].

Bimetallic Sn-platinoid electrodes have been a focus of alloy research due to the excellent electrocatalytic properties reported for pure Sn electrodes, which additionally present certain selectivity towards N_2 gas. On Sn-Pt alloy electrodes, Sn promotes effective electrocatalytic activity for NO_3^- reduction compared with pristine Pt electrodes [80,175]. The main gaseous product yielded with intermediate Sn coverage on Sn-Pt electrodes is N_2O, which can be further reduced to N_2 on free Pt sites [79,80]. High Sn coverage yields NO as main gaseous species, which is probably associated with the lower sorption of NO on Sn similar to the trend observed on Cu [51]. In contrast, Pd-Sn alloys
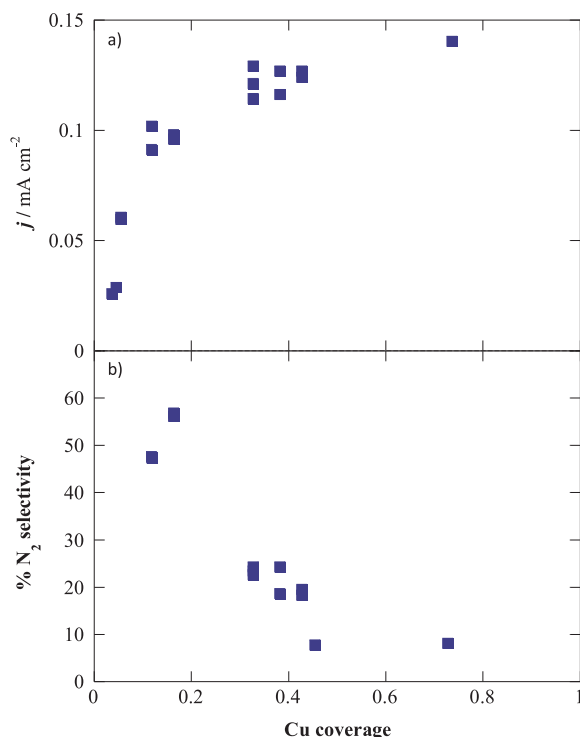
Fig. 12. Influence of Cu coverage of Cu-Pd alloys on (a) electrocatalytic activity and (b) selectivity towards N_2 during electrochemical reduction of 0.1 M NO_3^- at 0.02 V vs SHE at pH 13.7.
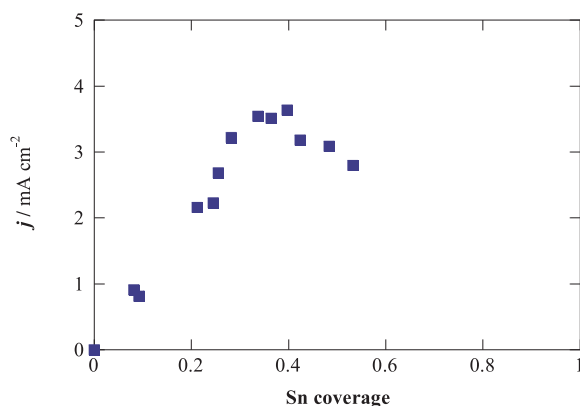Figure adapted from [173].

Fig. 13. Influence of Sn coverage of Pd-Sn alloys on electrocatalytic activity during electrochemical reduction of 0.1 M NO_3^- at –0.1 V vs SHE in 0.1 M $HClO_4$ solution.
Figure adapted from [79].

present similar behavior to Pt-Sn. The presence of Sn enhances nitrate reduction to nitrite [176–178], but excessive Sn coverage reduces the electrocatalytic activity [179,180] as depicted in Fig. 13. The dominant volatile species released is N_2O, which suggests that those electrodes may be as suitable as electrodes that produce N_2; however, N_2O is a potent greenhouse gas and may become a factor when considering sustainability of different nitrate removal systems.

4.1.3. Boron-doped diamond as high performance electrodes

Boron-doped diamond (BDD) is a very promising electrode material because of its excellent electrochemical properties: (i) wide working potential window; (ii) high stability, even under aggressive environments (e.g., high acid and alkaline media); (iii) corrosion-resistance; (iv) enhanced signal/background ratio; (v) low electrocatalytic
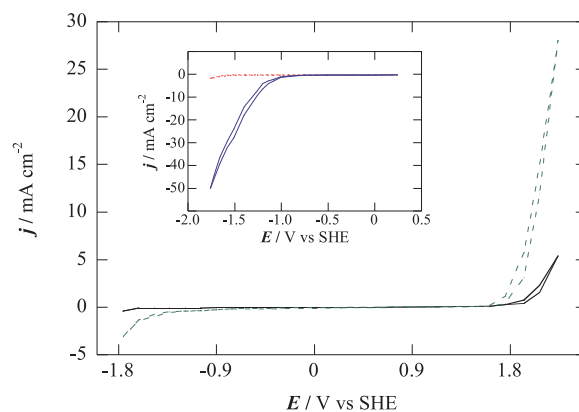

Fig. 14. Effect of boron doping on the electrochemical window as observed in cyclic voltammograms at scan rate 100 mV s^{-1} in 0.1 M KCl of polycrystalline boron doped diamond electrodes with different boron doping (solid black line) B/C = 2000 ppm and (dotted green line) B/C = 14,000 ppm. Inset panel shows the cyclic voltammogram of BDD B/C = 6000 ppm recorded at 100 mV s^{-1} in (dashed red line) 1.0 M KCl and 1.0 M $NaNO_3$ (solid blue line). (For interpretation of the references to colour in this figure legend, the reader is referred to the web version of this article).
Figures adapted from [186,187].

inhibition; and (v) modular properties depending the level on doping [181,182]. Since early publications in 1980 s, the uses for this versatile material have steadily increased and show electrochemical water treatment applications as one of the main research trends [28,183]. However, it is currently quite expensive (~ 10 \$ cm^{-2}).

Fujishima's group [58] first reported the application of diamond materials for electrochemical nitrate reduction. Based on continuous three-day long experiment, Tenne et al. [58] observed no changes in the electrode morphology and nitrate reduction performance. However, they also observed increases in Faradic Efficiency towards N_2 evolution, which reached 100% following a lag period before reduction initiated. This lag period suggests the presence of an autocatalytic mechanism (see Section 2.2), probably involving one of the reaction intermediates.

The low electron density in the conduction band, which is unusual for such a high-bandgap p-type material, could explain the high nitrate reduction efficiencies for BDD. This bandgap circumstance typically results in slow water reduction kinetics and a wider electrochemical window (see Fig. 14), which minimizes the competing effect caused by hydrogen evolution observed on other conventional electrode materials [58,184]. Specifically in the case of BDD, nitrate reduction is not exhibited at potentials that are more cathodic than –0.6 V, while H_2 evolution starts at –1.0 V and is fairly impeded until reaching values ca. –2.0 V [185,186].

After extended potentiostatic electrolysis (16 h) of nitrate solutions with BDD anodes, the ionic species distribution depends highly on the applied potential, as illustrated in Fig. 15. According to Lévy-Clément et al. [187], only N_2 products are generated when the cathode potential ranges between –1.5 V and –1.7 V. However, when the potential shifts to the –1.7 V to –2.0 V range, higher nitrate reduction is observed, which is also paralleled by higher nitrite yields. Ghazouni et al. [48] reported low accumulation of nitrite and ammonia after attaining 91% NO_3^- reduction (Fig. 15) when using BDD as cathode and anode. The high evolution of N-gases may be related to the ammonia oxidation by hydroxyl radicals [48,96], although experimental evidence of these mechanisms have not been reported and is thus an area for future research.

Electrocatalytic efficiencies for nitrate reduction on BDD is influenced by several factors, including boron doping, conductive support, grain size, and sp^3/sp^2 carbon ratio. Increasing boron doping of diamond electrodes from 200 to 14,000 ppm affects the electrochemical window width and the current density response, which improves charge
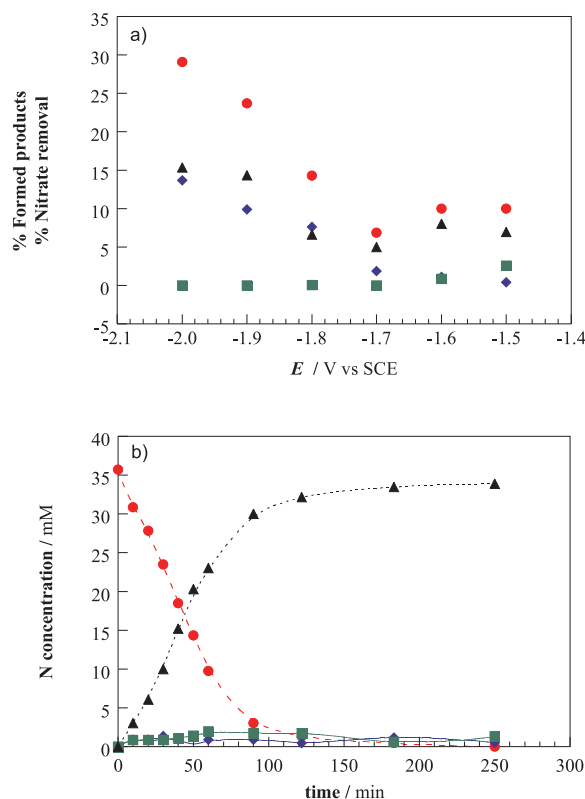
Fig. 15. (a) Distribution of by-products obtained after 16 h of potentiostatic electrolysis of 1 M KNO₃ with BDD cathode depending on the applied potential. (b) Concentration profiles of N-species during galvanostatic electrolysis of 35.7 mM NO_3^- with BDD cathode at 35.7 mA cm⁻². N-species: (●) NO_3^-, (◆) NO_2^-, (■) NH_4^+, (▲) N_2.
Figures adapted from [48,187].

transfer kinetics [186]. Selecting an adequate conductive support can enhance adsorption/interaction of nitrate with BDD surface, which results in a faster charge transfer reaction [184]. Matshushima et al. [188] studied the influence of the grain size of films grown at different growth times. BDD films grown at 5 h had small crystal size, larger surface area and higher roughness (see Fig. 16) than those grown at longer times such 10 h. However, films with larger grain size (10 h growth) presented higher sensitivity for nitrate reduction. This behavior is related to the decrease of sp² bonded carbon impurities at grain boundaries. The decrease of sp² carbon reduces oxygen termination and increases electron transfer kinetics on BDD surface as verified also by Fujishima's and Swain's groups [189,190]. Both effects (i.e., doping and crystal size) are closely related to one of the most influential characteristics recently identified: the sp³/sp² ratio [182]. The effect of sp³/sp² ratio has been discussed for organic pollutants electrochemical oxidation performance [191,192] and in electroanalysis sensitivity [181,193], but electrocatalytic nitrate reduction has not been reported. Therefore, this influential parameter must be studied to understand the capabilities of BDD electrodes and to evaluate the possible modulation of products selectivity during electrochemical nitrate reduction.

4.1.4. Carbonaceous composite electrodes for low-cost nitrate reduction

Carbonaceous electrodes are cheaper than precious metals. Unfortunately, weak electrocatalytic responses for NO_3^- reduction and slower kinetic rates have been observed [138,194]. Therefore, the use of pristine carbonaceous materials for nitrate removal has not been extensively reported.

Carbonaceous materials for electrochemical nitrate reduction are primarily used in composite electrodes as support for electrocatalytic nanoparticles of materials discussed above. Composite electrodes are designed to reduce material costs while enhancing the nitrate reduction kinetics. The use of nanoparticles is paramount to provide high catalytic surface of highly expensive noble/platinoid metals and alloys with lower mass requirements (see Table 1). Nanoparticles are usually immobilized on cheaper and stable conductive materials (e.g.,
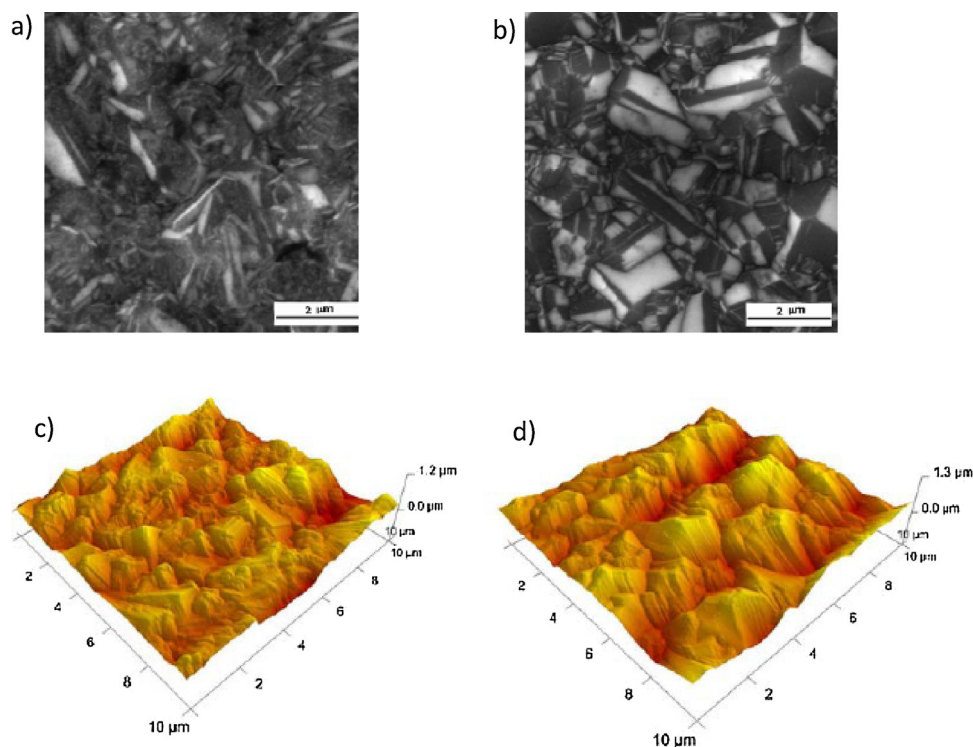

Fig. 16. (a,b) SEM and (c,d) AFM images of boron-doped diamond grown by thin films hot filament assisted chemical vapor deposition for (a,c) 5 h and (a,d) 10 h. Adapted from [188].

carbonaceous substrates such as graphite [195,196], glassy carbon [197,198], activated carbon [199], carbon cloth [200], carbon fiber [32], carbon nanotubes [201,202], mesoporous carbon [133] or graphene [203]). An emerging question that needs to be addressed prior commercialization is the electrode stability and nanoparticle leaching to define operational life and to identify health risks [204].

4.2. Crystal planes influences on products selectivity

Crystal planes play a key role in selectivity and catalytic activity of reactions because they define the arrangement of atoms on the interfacial surface where heterogeneous reactions occur. This could be an important factor that facilitates or inhibits reduction kinetics because nitrate reduction is a structure-sensitive reaction as demonstrated on single-crystal platinum electrodes [50,205]. However, the kinetics are also controlled by other competitive species interaction with the surface (e.g., hydrogen, sulfate, and others). The different electrocatalytic response of single crystal Pt electrodes with defined Miller index planes Pt (5 5 4), Pt(5 5 3), Pt(1 1 1), Pt(1 1 0), Pt(1 0 0) indicate a strong influence of the preferential crystalline planes on the nitrate reduction rates. Similar influence of crystal planes on reactivity has been observed in other metals like Cu, where crystallographic planes Cu(1 1 1) presented improved reduction rates in comparison to Cu(1 0 0) [206].

In addition to crystallinity, surface steps density also affects electrocatalytic nitrate adsorption and reduction. Taguchi and Feliu [101] reported an increase in electrocatalytic activity with the increase of the step density on Pt[n(1 1 1)×(1 1 1)] surfaces. This study inferred that NO_3^- does not adsorb on the (1 1 1) terrace sites, but it does adsorb on the step sites before it is reduced in the H_2 adsorption region of potential. Surface steps density has not been significantly explored for nitrate removal.

Preferential crystal planes have the ability to enhance selectivity towards the desired N_2 [84]. Terraces (1 0 0), for example, drive the process towards the N_2 selectivity by enhancing the above-discussed Duca-Feliu-Koper mechanism (see Fig. 5). Defects in symmetry have the potential to dramatically reduce N_2 evolution at [(1 0 0) x (1 1 0)] and [(1 0 0) x (1 1 1)] surfaces. In contrast, the use of nanoparticles with preferential (1 0 0) surfaces could considerably improve selectivity.

Better understanding the role of crystalline planes could significantly promote the development of tailored nitrate-reducing technologies, especially because today's technologies allow for controlled fabrication of nanomaterials that exhibit desired crystalline planes. Consequently, N_2 selectivity could be enhanced by manufacturing engineered nanoparticles with targeted preferential crystallographic planes orientation and then using them to nano-enable the composite electrodes.

4.3. Tridimensional electrodes as a strategy to minimize mass transfer limitation

Mass transport of nitrate in solution to electrode surfaces and diffusion of by-products off the electrode surface are a major rate-limiting process in electrochemical nitrate reduction. Increasing electrode surface area naturally facilitates faster nitrate reduction.

Fig. 17 illustrates a tridimensional porous $Cu_{70}Ni_{30}$ alloy cathode that allows the solution to pass through it, which enables more electrodic surface (higher surface area) to be in contact with the electrolyzed solution enhancing mass transport. Nanowires are another form of tridimensional electrodes. However, nanowires cannot be used directly and must be embedded in a composite systems [207]. Jha et al. [208] found that operational times can be severely reduced by three-fold and Faradaic efficiencies doubled when using tri-dimensional electrodes (62 h and 80% efficiency at 0.25 A cm^{-2}) in comparison to planar electrodes (200 h and 30% efficiency at 0.25 A cm^{-2}). This can be related to the larger currents observed in voltammetric analysis of diffusion controlled processes when using tridimensional and porous
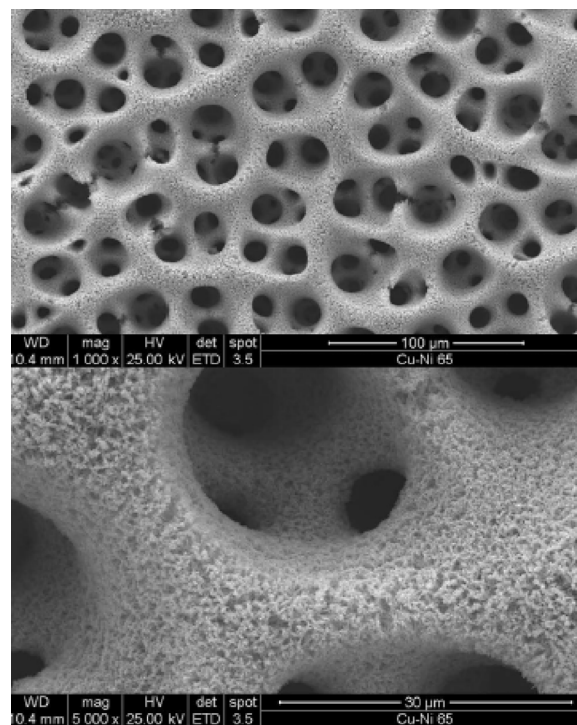

Fig. 17. SEM images of a tridimensional porous $Cu_{70}Ni_{30}$ cathode used on the electrochemical reduction of nitrate to improve mass transfer. Figure adapted from [219].

cathodes [170]. When more chemical species react at the electrode surface, the current response is higher. Tridimensional electrodes have not been explored for nitrate reduction catalysis and should be evaluated against conventional plate cathodes.

4.4. Influence of electrolytes and redox mediators on the electrochemical reduction kinetics

Electrolytes in solution with nitrate can significantly influence nitrate reduction rates. Increasing concentration of certain anions decreases the electrocatalytic nitrate reduction by competing for surface adsorption sites or influencing the magnitude of electrostatic hindering effects, which are governed by characteristic enthalpy of sorption of each anion on specific metal cathodes. For example, the electrocatalytic response of Pt, Cu and Ag is considerably higher in presence of ClO_4^- than SO_4^{2} because ClO_4^- (an inert electrolyte) is very low adsorption while SO_4^{2-} competes with NO_3^- for surface adsorption sites [51]. Sulfate also inhibits other pollutant reduction for Ir, Ru, Rh, Au or Pd electrodes [51]. Competition among different anions for surface adsorption sites is unique to each metal-anion pair.

Some inorganic pollutants in water can be removed via electrochemical processes but may interfere with targeted nitrate removal from water. Hexavalent chromium (Cr(VI)) is a carcinogenic pollutant in groundwater at parts-per-billion levels, due to both natural geological or anthropogenic sources [209]. During the reduction of Cr(VI) to trivalent chromium according to Reaction (60), Duarte et al. [154] observed that a chromium hydroxide layer formed on the Ni cathode surface that acts as an insulator and prevents the transfer of reducing electrons. This insulator layer virtually stops the electrocatalytic reduction of nitrate at parts-per-million hexavalent chromium concentrations. However, this undesired side-effect can be minimized or completely avoided by intermittently reversing the polarity of the electrodes.

$$CrO_4^{2-} + 4 H_2O + e- \rightarrow Cr(OH)_{3(s)} + 5 OH^- \qquad (60)$$
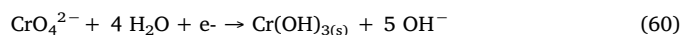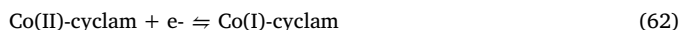
In contrast, Katsounaros et al. [75] reported no inhibition of nitrate reduction by Cr(VI) when Sn cathodes were used because of the very negative potentials during operating conditions. At very negative potentials, complete Cr(VI) reduction occurred and deposited elemental chromium on the electrode surface instead Cr(OH)$_{3(s)}$. The long-term effect on electrochemical performance of undesired Cr electrodeposits was not evaluated. Nevertheless, this should result in the simultaneous removal of chromium and nitrate by electrochemical reduction. Even though this dual application is not addressed in the literature, electrodes fouled with Cr(OH)$_3$ and other chromium-reduced species can be cleaned by reversing polarity or cleaning with acid solutions.

The effects of alkali and alkaline cationic species on nitrate reduction process have been barely studied, but two main effects emerge. First, cations act as proton donors, i.e., protons that are required in the nitrate electrochemical reduction as discussed in the mechanisms of Fig. 5. Ogawa et al. [42] observed a linear relationship between the nitrate reduction potential and the logarithm of the first hydrolysis constant (*K_1) of metal cations (e.g., p*K_1 = 5.0 for Al^{3+} + H$_2$O → AlOH^{2+} + H$^+$ [210]). Hydrolysis of metal ions near the electrode surface supplies the required protons for nitrate reduction [52,211]. Second, the presence of cations suppresses the electrostatic repulsion forces between the cathode and nitrate (both negatively charged) by providing balancing positive charge centers and forming a neutral ion pair according to Reaction (61). Katsounaros et al. [52] showed that nitrate reduction increased for different alkali metals, with lithium having less of an impact than cesium (Li$^+$ < Na$^+$ < K$^+$ < Cs$^+$). This sequence correlates well with the increasing values of the nitrate association constants for Li$^+$, Na$^+$, K$^+$ and Cs$^+$, which are 0.65, 1.43, 2.04 and 2.35, respectively. Therefore, higher association constants between cations and nitrate appear correlated with faster reduction kinetics, which may be due to the higher suppression of the electrostatic repulsion.

$$M^+ + NO_3^- \leftrightharpoons M\cdots NO_3 \tag{61}$$

Some electrolytes behave as redox mediators propagating indirect electrochemical reactions that can enhance nitrate reduction rates. Redox mediators mediate between the direct charge transfer process at the electrode surface and nitrate reduction. Different cationic species have been considered in literature such as Yb(III)-Yb(II) couple, Zr(IV), Hf(IV) and La(III) [41,42]. These ionic metals act as intermediary species for the charge transfer from the electrode to nitrate ion, thus allowing nitrate reduction at more positive potentials. However, redox mediators remain in solution. While not reported to be toxic, their use in drinking water may be questioned by regulators. In addition, chemicals serving as redox mediators are expensive and thus may not be practical for continuous addition at water treatment plants.

Affixing redox mediators on electrode surfaces could be an alternative strategy to overcome their use in solution. For example, cobalt-organic complexes (e.g., cobalt-cyclam or cobalt-protoporphyrin) represent interesting fixed-redox approach [212,213]. The cobalt-organic mediated mechanism can be summarized as follows:

$$\text{Co(II)-cyclam} + e\text{-} \leftrightharpoons \text{Co(I)-cyclam} \tag{62}$$

$$\text{Co(I)-cyclam} + NO_3^- \rightarrow \text{Co(III)-cyclam} + NO_2^- \tag{63}$$

Affixing redox mediators to cathodes should promote indirect electrochemical nitrate reduction on other inert electrodes. However, rate-limiting factors associated with diffusion of nitrate would persist. Moreover, concerns related to the stability and possible leaching of heavy metals (e.g., cobalt ions) into drinking water is a potential barrier without careful studies to validate long-term performance and continued attachment to electrode surfaces.

4.5. Dissolved oxygen effects on nitrate reduction

The presence of dissolved oxygen in solution is important in developing efficient nitrate reduction technologies. Dissolved oxygen is present below saturation levels (i.e., 1 to 8 mg/L) in groundwaters containing nitrate, otherwise ammonia would likely be present in anoxic conditions. Additionally, oxygen is continuously electrogenerated from water oxidation at the anode. Oxygen can be reduced at the highly cathodic potentials required for nitrate electrochemical reduction. Consequently, oxygen reduction to hydrogen peroxide (64) and the complete reduction to water (65) occur at the cathode at the applied potentials required for nitrate reduction (e.g., Fig. 4):

$$O_2 + 2\,e\text{-} + 4\,H^+ \rightarrow H_2O_2 \tag{64}$$

$$O_2 + 4\,e\text{-} + 4\,H^+ \rightarrow 2\,H_2O \tag{65}$$

The current efficiency of nitrate reduction decreases in presence of oxygen [44]. However for small contents of O$_2$ in solution, slightly higher removal percentages are attained. According to control experiments conducted by Li et al. [44], the slight removal of nitrate could not be related to redox reactions with H$_2$O$_2$, but it would be related to catalytic role of other reactive oxygen species such as superoxide radical (O$_2\cdot^-$). The influence of dissolved oxygen is barely addressed in research. Understanding the impact of dissolved oxygen on electrochemical nitrate reduction would contribute to design strategies that minimize oxygen-related competition and improve conversion rates.

4.6. Effect of pH on products selectivity and kinetics

Electrochemical nitrate reduction can occur over a wide pH range, with studies conducted from highly acidic [96,214] to highly alkaline conditions [48,170]. The hydrogen evolution reaction is pH-dependent according to Nernst equation (Fig. 4b). Furthermore, the hydrogen evolution reaction competes (i.e., consumes electrons) with nitrate for electrochemical reduction. Faradaic efficiencies of hydrogen evolution are higher in acid media than in alkaline media. Consequently, hydrogen evolution can reduce the Faradaic efficiencies of nitrate reduction in acidic media [196,215]. The direct charge transfer process is less effective because of the competition with hydrogen. However, the indirect electrochemical autocatalytic processes (Vetter and/or Schmid) in acidic media may compensate this undesired effect [54] increasing the reduction kinetics. In contrast, as illustrated in Fig. 5, the rate-limiting step and the following reduction steps described for the electrochemical nitrate reduction mechanism consume protons during the reduction process. This correlates well with the pH increase observed during the electrochemical nitrate reduction [36]. For example, Rajmohan reported a significant change from pH 1 to pH > 7 in non-buffered water [141]. The alkalinization of treated effluent could limit electrochemical technologies in decentralized treatment applications (e.g., POU). Xing et al. [216] pointed out from batch experiments that under low H$^+$ availability (alkaline conditions), the reduction process yields mainly nitrite from nitrate, whereas higher proton concentrations (more acidic conditions) may yield reduction products (N$_2$, N$_2$O, NH$_4^+$, etc.) beyond nitrite step. However, batch electrolysis in alkaline media demonstrated complete reduction to ammonia and other species [48,170]. During electrochemical nitrate reduction on Pt/Sn electrodes, Koper's group observed NO was the main gaseous products at pH 1, whereas N$_2$ gas was the main gaseous species evolved at pH > 3.6, and the overall rate of nitrate loss was slower at higher pH [80]. There is a need to conduct experiments in continuous flow systems to assess pH fluctuations as a function of nitrate removal on different electrodic materials at ambient and reduced pH levels and with addition of sulfuric or other common water treatment acids.

5. Electrocatalytic reduction of nitrate in waste and drinking waters

Many studies apply electrochemical nitrate treatment to groundwaters or wastewaters containing a range of nitrate concentrations, pH

and electrode materials. Complete nitrate removal (1.8 M NO_3^- or 25.2 g N L^{-1}) in a nuclear waste achieved > 70% selectivity towards N_2 using Bi and Sn cathodes after 7 h of treatment at 450 mA cm^{-2} and an energy consumption of 10.1 kW h g^{-1} of N [45]. Bockris and Kim [39] reported complete reduction of nitrate (1.95 M or 27.3 g N L^{-1}) and nitrite (0.66 M or 9.24 g N L^{-1}) with nickel cathodes in different divided cell designs and an electrical requirement of 2.1 kW h g^{-1} of N treating 2.5×10^4 L daily.

Electrochemical processes are versatile and scalable. With six nitrate-polluted groundwater sources in Ho Chi Minh City (Vietnam), electrochemical reduction with copper and polypyrrole/Cu cathodes under potentiostatic conditions (–0.70 V vs Ag/AgCl) achieved ∼10% nitrate removal and ∼50% of nitrite formation after five hours of operation [217]. These groundwaters contained low nitrate concentrations (4 to 15 mg N L^{-1}), which likely resulted in low concentration gradients to the electrode surface and hence limited nitrate mass transfer. Additionally, the potentiostatic working conditions employed did not accelerate the electrokinetics as expected from the low current responses observed for sluggish reaction in a complex water matrix. Another constraint is related to the lower performance of polypyrrole/Cu cathodes in comparison to Pd-Cu or Pd-Sn composite electrodes. To overcome this later barrier, Ghazouani et al. [48] reported higher nitrogen removal by using a bipolar electrochemical cell with BDD electrodes at constant current density of 35.7 mA cm^{-2}; 85% reduction in human urine, 67% reduction in municipal wastewater and 64% reduction in slaughterhouse effluent were attained with energy consumption of 35.5 kW h g^{-1} of N, 25.8 kW h g^{-1} of N and 23.4 kW h g^{-1} of N, respectively. Note that this higher energy requirement is associated with the considerably lower concentrations of NO_3^- in these effluents corresponding to 6.16 mg N L^{-1} in urine, 8.18 mg N L^{-1} in municipal wastewater and 9.74 mg N L^{-1} in slaughterhouse effluent.

One of the limiting factors is the requirement of certain conductivity to perform electrolytic processes. Even though the influence of conductivity is not considered in literature, low conductivities may increase operational cost due to the solution resistance. Electrochemical nitrate reduction combined with conventional physical water treatment technologies can improve current efficiencies and treatment performance. Ion exchange is widely applied to separate NO_3^- at low concentrations from water. After regeneration of ion exchange columns, high NO_3^- levels exist in the brine regenerate solution. Applying electrochemical processes to remove nitrate in the brine can extend the life of the brines and reduce disposal costs [36,104]. The high nitrate concentration is beneficial to ensure greater faradaic efficiencies, although the main challenge is associated with the selectivity towards N_2 in divided electrochemical cells [159]. However, high ionic strength present in the brines, which contain 5% to 20% sodium chloride, likely presents lower ohmic resistance and consequently lower energy consumption. This may be dwarfed by the competition effect between electrolytes for the electrode surface. Undivided electrochemical cells would benefit from the high chloride concentration that enhances electrochlorination process to yield N_2 as final product [131,132]. This type of combination of ionic exchange/electrocatalytic denitrification is a treatment approved by the UK Drinking Water Inspectorate [104]. Commercial systems for this type of brine treatment already exist as shown schematically in Fig. 18 and using electrochemical filter press cells as shown in Fig. 19. These systems enable consistent nitrate electrochemical reduction in consecutive cycles and achieve complete nitrate removal at system flow rates of 216 m^3 h^{-1} and influent ground water with 70 mg L^{-1} NO_3^-. The complete removal of nitrate allows brine reutilization in several consecutive cycles. The integrated process can remove 114 kg day^{-1} of NO_3^- consuming 1.58 kW h g^{-1} of N, 115 Kg of NaCl and 0.17 m^3 of 35% HCl and has an average operating cost including labor of $0.13 per m^3, which is only a fraction of the $0.5-2.0/1000 gal cost to treat most drinking waters.

6. Key insights

Studies of electrochemical nitrate reduction in drinking waters have been increasingly reported (Fig. 1), yet there appears no consensus on the optimal electrode material for continuous flow reactors. The electrochemical reduction process involves various intermediates and products (NO_2^-/HNO_2, NH_3/NH_4^+, N_2O and N_2). For water treatment, the desired end product is N_2 because NO_2^- and NH_4^+ pose health, aesthetic and operational problems. The key rate-limiting step is nitrate reduction to nitrite, which is influenced by mass transfer from the bulk water to the electrode surface, the adsorption of nitrate on the electrode surface, and electron transfer.

Electrode material affects both the kinetics and product selectivity during electrochemical nitrate reduction. Metals with highly occupied d-orbitals (e.g., Cu, Ag, Pt) and unclosed d-orbital shells are ideal for electrochemical nitrate reduction because they have an energy level similar to nitrate's LUMO π* that allows for facilitated first electron transfer. Among these metals, copper exhibits both the highest electrocatalytic kinetics and the lowest cost. However, copper cathodes in water treatment may be limited due to lack of stability (corrosion and leaching) and because they generate ammonia as the main by-product. Conversely, platinum and palladium electrodes offer high N_2 selectivity but low nitrate reduction kinetics due to competitive hydrogen evolution from water reduction at the electrode surface.

Metal alloys present an opportunity because preferential performance characteristics of different metals can be combined into one electrode material. Two main opportunities were identified for working with copper. First, Pt-Cu and Pd-Cu alloys improve performance when compared to pure electrodes due to the synergy between high N_2 selectivity of Pt/Pd and quick NO_3^- reduction kinetics of Cu. Second, cupronickels exhibit increased resistance to corrosion and greater stability compared with copper electrodes, making these electrodes competitive for the electrochemical nitrate reduction in brines with high Cl^- concentration.

Nano-enabling composite electrodes may enhance kinetics in electrochemical nitrate reduction by increasing electrode surface area. Controlled manufacturing of engineered nanoparticles with targeted preferential crystallographic planes (e.g., Pt(1 0 0)) can improve the adsorption density and selectivity of the electrode. The use of nanoparticles as electrocatalysts may enhance development of nitrate reducing technologies.

The kinetics and selectivity of the electrochemical nitrate reduction are affected by water quality, pH, dissolved oxygen, ionic strength, chloride and electrode geometry. Acidic pH favors NO_2^- reduction but may increase electrode corrosion. The pH can also influence the reaction potential and the relevance of competing reactions. Significantly more attention should be given to this parameter because the effects may vary based on the electrode material. Dissolved oxygen influences nitrate reduction kinetics by forming superoxide radical ($O_2 \cdot^-$), which competes with nitrate for cathodic reduction. Better understanding of the mechanistic influence of oxygen could improve conversion rates by controlling oxygen in reactors. Tridimensional electrode geometries can reduce operational times by three-fold, thus reducing the mass transfer limitation and increasing electrode surface area.

Hydrogen production during electrochemical nitrate reduction occurs, yet reports are mixed regarding its net effect on nitrate reduction kinetics. Hydrogen adsorption can compete for cathodic reduction of the electrochemical cell and inhibit nitrate reduction. However, adsorbed hydrogen also creates a reducing environment in the hydrogen evolution region. Here, NO_2^- and NO species can react with the $H_{(ad)}$ and increase the kinetics. Reliable experiments are needed to clearly state the involvement of the hydrogenation on the reduction of nitrate, which could become a research nexus between electrochemical and hydrogen catalytic technologies.

Simultaneous reactions can be beneficial. Electrochlorination can benefit from the anodic oxidation of chloride to chlorine and nitrate
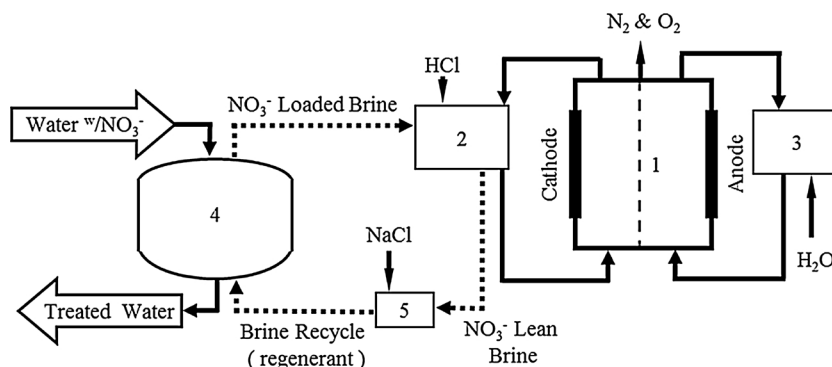
Fig. 18. Diagram of De Nora® electrochemical nitrate reduction from ionic exchange brine generation. Components present in the full scale system include: (1) the separate compartment electrochemical cell, (2) catholyte reservoir, (3) anolyte reservoir, (4) ion exchange column, and (5) regenerate brine feed tank.

Fig. 19. Commercial electrolyzer and piping of the NitroCat-ZLD™ integrated process from De Nora® used on the electrochemical reduction of nitrate in brine.

reduction to ammonia. Concurrently, chlorine oxidizes ammonia to N_2. The formation of chloramines as intermediates could be an added value of the electrochemical reduction process, which in one step would: (i) produce *in situ* disinfectant species required in drinking water applications and (ii) reduce the content of nitrate in water by transformative technologies with non-added chemicals. Electrochlorination allows for various ammonia selective electrodes (e.g., cupronickel) to remain as competitive and cheaper materials for the electrochemical nitrate reduction. While mechanistic models exist, there are no process models currently available for electrochemical reduction of NO_3^- in continuous flow systems. These models would help optimize electrochemical device application and minimize E_{EO} requirements.

There is a need to evaluate various electrodes in single-pass continuous flow electrocatalytic reactors under a range of expected simulates water qualities, such as those suggested by NSF International. Three full-scale applications exist, and each offers different challenges. First, point-of-use systems treating groundwater at private residences

may operate intermittently and have a wide range of influent water conditions, including presence of iron or other metals that may affect electrode surfaces. In such applications, there is no opportunity for pH adjustment, and this could affect by-product formation. Robust electrode and operating configurations would be required. Second, small communities treating groundwater that contains nitrate at 10–50 mg NO_3-N L^{-1} will likely want to avoid addition of acids and bases but would likely already add chlorine. Thus, there may be opportunities to take advantage of chloramine formation if ammonia is produced during the nitrate reduction process. The third—and perhaps the best—entry point for electrocatalytic nitrate reduction would be using the process to treat ion exchange brines in a batch process. As nitrate accumulates in brines (> 1 g NO_3-N L^{-1}), the rates and by-product selectivity improve, and it is feasible to add acids to depress pH or chloride to produce chloramine intermediates. Treating nitrate in ion exchange brines could increase the brine lifetime by $> 10x$, until high levels of sulfate or other ions may limit the ability to regenerate the ion exchange resins.

References

[1] E.E. Stüeken, M.A. Kipp, M.C. Koehler, R. Buick, The evolution of earth's bio-geochemical nitrogen cycle, Earth-Sci. Rev. 160 (2016) 220–239, http://dx.doi.org/10.1016/j.earscirev.2016.07.007.

[2] A. Menció, J. Mas-Pla, N. Otero, O. Regàs, M. Boy-Roura, R. Puig, J. Bach, C. Domènech, M. Zamorano, D. Brusi, A. Folch, Nitrate pollution of groundwater; All right.. ., but nothing else? Sci. Total Environ. 539 (2016) 241–251, http://dx.doi.org/10.1016/j.scitotenv.2015.08.151.

[3] Y.Y. Yang, G.S. Toor, Sources and mechanisms of nitrate and orthophosphate transport in urban stormwater runoff from residential catchments, Water Res. 112 (2017) 176–184, http://dx.doi.org/10.1016/j.watres.2017.01.039.

[4] M.R. Burkart, J.D. Stoner, Nitrate in aquifers beneath agricultural systems, Water Sci. Technol. 56 (2007) 59–69, http://dx.doi.org/10.2166/wst.2007.436.

[5] M.G. Rupert, Decadal-scale changes of nitrate in ground water of the United States, 1988–2004, J. Environ. Qual. 37 (2008) S240–S248, http://dx.doi.org/10.2134/jeq2007.0055.

[6] K.R. Burow, B.T. Nolan, M.G. Rupert, N.M. Dubrovsky, Nitrate in groundwater of the United States, 1991–2003, Environ. Sci. Technol. 44 (2010) 4988–4997, http://dx.doi.org/10.1021/es100546y.

[7] B.M. Afzal, Drinking water and women's health, J. Midwifery Women's Health 51 (1980) 12–18, http://dx.doi.org/10.1016/j.jmwh.2005.08.014.

[8] G.C. NAE, Manage the Nitrogen Cycle, (2017) Http://www.engineeringchallenges.org/challenges/nitrogen.aspx.

[9] R.C. Sobti, S.K. Sharma, Archina, nitrate removal from ground water, Water Res. 9 (2011) 1667–1675, http://dx.doi.org/10.1016/S0043-1354(87)80018-0.

[10] B.A. Kapoor, T. Viraraghavan, Nitrate removal from drinking water—review, J. Environ. Eng. 123 (1997) 371–380, http://dx.doi.org/10.1061/(ASCE)0733-9372(1997)123:4(371).

[11] M.H. Ward, T.M. deKok, P. Levallois, J. Brender, G. Gulis, B.T. Nolan, J. VanDerslice, Workgroup report: drinking-water nitrate and health - recent

findings and research needs, Environ. Health Perspect. 113 (2005) 1607–1614, http://dx.doi.org/10.1289/ehp.8043.

[12] A.M. Fan, V.E. Steinberg, Health implications of nitrate and nitrite in drinking water: an update on methemoglobinemia occurrence and reproductive and developmental toxicity, Regul. Toxicol. Pharmacol. 23 (1996) 35–43, http://dx.doi.org/10.1006/rtph.1996.0006.

[13] J. Pelley, Nitrate eyed as endocrine disrupter, Environ. Sci. Technol. 37 (2003) 162A, http://dx.doi.org/10.1021/es032437n.

[14] P.J. Weyer, J.R. Kantamneni, X. Lu, M.H. Ward, J.R. Cerhan, Nitrateingestion from drinking water and diet and cancer risk, Epidemiology 19 (2009) S55, http://dx.doi.org/10.1097/01.ede.0000339692.47203.99.

[15] WHO, Nitrate and Nitrite in Drinking-Water, (2016).

[16] USEPA, Ground Water and Drinking Water Table of Regulated Drinking Water Contaminants, (2017) Https://www.epa.gov/ground-Water-and-Drinking-Water/table-Regulated-Drinking-Water-Contaminants.

[17] M.J. Pennino, J.E. Compton, S.G. Leibowitz, Trends in drinking water nitrate violations across the United States, Environ. Sci. Technol. 51 (2017) 13450–13460, http://dx.doi.org/10.1021/acs.est.7b04269.

[18] Y. Zhai, Y. Lei, J. Wu, Y. Teng, J. Wang, X. Zhao, X. Pan, Does the groundwater nitrate pollution in China pose a risk to human health? A critical review of published data, Environ. Sci. Pollut. Res. 24 (2017) 3640–3653, http://dx.doi.org/10.1007/s11356-016-8088-9.

[19] D. Han, M.J. Currell, G. Cao, Deep challenges for China's war on water pollution, Environ. Pollut. 218 (2016) 1222–1233, http://dx.doi.org/10.1016/j.envpol.2016.08.078.

[20] K. Parris, Impact of agriculture on water pollution in OECD countries: recent trends and future prospects, Int. J. Water Resour. Dev. 27 (2011) 33–52, http://dx.doi.org/10.1080/07900627.2010.531898.

[21] R.C. Hamme, S.R. Emerson, The solubility of neon, nitrogen and argon in distilled water and seawater, Deep Res. Part I Oceanogr. Res. Pap. 51 (2004) 1517–1528, http://dx.doi.org/10.1016/j.dsr.2004.06.009.

[22] A.J. Bard, L.R. Faulkner, Electrochemical Methods. Fundamentals and Applications, 2nd edition, Wiley, New York, 2001, http://dx.doi.org/10.1016/B978-0-12-381373-2.00056-9.

[23] Z. Mácová, K. Bouzek, J. Šerák, Electrocatalytic activity of copper alloys for NO3- reduction in a weakly alkaline solution, J. Appl. Electrochem. 37 (2007) 557–566, http://dx.doi.org/10.1007/s10800-006-9287-8.

[24] I. Haque, M. Tariq, Voltammetry of nitrate at solid cathodes, ECS Trans. 16 (2009) 25–33.

[25] L. Szpyrkowicz, S. Daniele, M. Radaelli, S. Specchia, Removal of NO3- from water by electrochemical reduction in different reactor configurations, Appl. Catal. B: Environ. 66 (2006) 40–50, http://dx.doi.org/10.1016/j.apcatb.2006.02.020.

[26] W. Li, C. Xiao, Y. Zhao, Q. Zhao, R. Fan, J. Xue, Electrochemical reduction of high-concentrated nitrate using Ti/TiO2 nanotube array anode and Fe cathode in dual-chamber cell, Catal. Lett. 146 (2016) 2585–2595, http://dx.doi.org/10.1007/s10562-016-1894-3.

[27] J.R. Bolton, K.G. Bircher, W. Tumas, C.A. Tolman, Figures-of-merit for the technical development and application of advanced oxidation technologies for both electric- and solar-driven systems (IUPAC technical report), Pure Appl. Chem. 73 (2001) 627–637, http://dx.doi.org/10.1351/pac200173040627.

[28] M. Lanzarini-Lopes, S. Garcia-Segura, K. Hristovski, P. Westerhoff, Electrical energy per order and current efficiency for electrochemical oxidation of p -chlorobenzoic acid with boron-doped diamond anode, Chemosphere 188 (2017) 304–311, http://dx.doi.org/10.1016/j.chemosphere.2017.08.145.

[29] K.J. Vetter, Electrochemical kinetics, Chapter 2, The Theory of Overvoltage, 1st ed., Academic Press, New York, 1967, http://dx.doi.org/10.1016/B978-1-4832-2936-2.50006-8.

[30] H. Huang, M. Zhao, X. Xing, I.T. Bae, D. Scherson, In-situ infrared studies of the Cd-UPD mediated reduction of nitrate on gold, J. Electroanal. Chem. 293 (1990) 279–284.

[31] M.C.P.M. da Cunha, M. Weber, F.C. Nart, On the adsorption and reduction of NO3- ions at Au and Pt electrodes studied by in situ FTIR spectroscopy, J. Electroanal. Chem. 414 (1996) 163–170, http://dx.doi.org/10.1016/0022-0728(96)04697-9.

[32] D. De, E.E. Kalu, P.P. Tarjan, J.D. Englehardt, Kinetic studies of the electrochemical treatment of nitrate and nitrite ions on iridium-modified carbon fiber electrodes, Chem. Eng. Technol. 27 (2004) 56–64, http://dx.doi.org/10.1002/ceat.200401832.

[33] F.F. Rivera, C.P. De León, J.L. Nava, F.C. Walsh, The filter-press FM01-LC laboratory flow reactor and its applications, Electrochim. Acta 163 (2015) 338–354, http://dx.doi.org/10.1016/j.electacta.2015.02.179.

[34] M. Paidar, K. Bouzek, H. Bergmann, Influence of cell construction on the electrochemical reduction of nitrate, Chem. Eng. J. 85 (2002) 99–109, http://dx.doi.org/10.1016/S1385-8947(01)00158-9.

[35] D. Pletcher, F.C. Walsh, Industrial Electrochemistry, Chapman and Hall, London, 1990.

[36] M. Paidar, I. Roušar, K. Bouzek, Electrochemical removal of nitrate ions in waste solutions after regeneration of ion exchange columns, J. Appl. Electrochem. 29 (1999) 611–617, http://dx.doi.org/10.1023/A:1026423218899.

[37] T.Y. Zhang, Y.L. Lin, B. Xu, T. Cheng, S.J. Xia, W.H. Chu, N.Y. Gao, Formation of organic chloramines during chlor(am)ination and UV/chlor(am)ination of algae organic matter in drinking water, Water Res. 103 (2016) 189–196, http://dx.doi.org/10.1016/j.watres.2016.07.036.

[38] H. Lan, X. Liu, H. Liu, R. Liu, C. Hu, J. Qu, Efficient nitrate reduction in a fluidized electrochemical reactor promoted by Pd-Sn/AC particles, Catal. Lett. 146 (2016) 91–99, http://dx.doi.org/10.1007/s10562-015-1615-3.

[39] J.O. Bockris, J. Kim, Electrochemical treatment of low-level nuclear wastes, J. Appl. Electrochem. 27 (1997) 623–634, http://dx.doi.org/10.1023/A:1018419316870.

[40] N.H. Kvaelsofaktioeselskab, Electrolysis of aqueous solutions with electrodes capable of being attacked, such as iron electrodes, Chem. Abstr. 15 (1921) 2038.

[41] S.W. Boese, V.S. Archer, Electrochemical reduction of nitrate in the presence of ytterbium(III), J. Electroanal. Chem. 138 (1982) 273–294.

[42] N. Ogawa, S. Ikeda, On the electrochemical reduction of nitrate ion in the presence of various metal ions, Anal. Sci. 7 (1991) 1681–1684.

[43] G. Horányi, E.M. Rizmayer, Electrocatalytic reduction of NO2- and NO3- ions at a platinized platinum electrode in alkaline medium, J. Electroanal. Chem. 188 (1985) 265–272, http://dx.doi.org/10.1016/S0022-0728(85)80067-X.

[44] H.-L. Li, D.H. Robertson, J.Q. Chambers, D. Hobbs, Electrochemical reduction of nitrate and nitrite in concentrated sodium hydroxide at platinum and nickel electrodes, J. Electrochem. Soc. 135 (1988) 1154–1158.

[45] I. Katsounaros, M. Dortsiou, G. Kyriacou, Electrochemical reduction of nitrate and nitrite in simulated liquid nuclear wastes, J. Hazard. Mater. 171 (2009) 323–327, http://dx.doi.org/10.1016/j.jhazmat.2009.06.005.

[46] B.P. Dash, S. Chaudhari, Electrochemical denitrificaton of simulated ground water, Water Res. 39 (2005) 4065–4072, http://dx.doi.org/10.1016/j.watres.2005.07.032.

[47] M.L. Bosko, M.A.S. Rodrigues, J.Z. Ferreira, E.E. Miró, A.M. Bernardes, Nitrate reduction of brines from water desalination plants by membrane electrolysis, J. Membr. Sci. 451 (2014) 276–284, http://dx.doi.org/10.1016/j.memsci.2013.10.004.

[48] M. Ghazouani, H. Akrout, L. Bousselmi, Nitrate and carbon matter removals from real effluents using Si/BDD electrode, Environ. Sci. Pollut. Res. 24 (2017) 9895–9906, http://dx.doi.org/10.1007/s11356-016-7563-7.

[49] D. Xu, Y. Li, L. Yin, Y. Ji, J. Niu, Y. Yu, Electrochemical removal of nitrate in industrial wastewater, Front. Environ. Sci. Eng. 12 (2018) 9, http://dx.doi.org/10.1007/s11783-018-1033-z.

[50] G.E. Dima, G.L. Beltramo, M.T.M. Koper, Nitrate reduction on single-crystal platinum electrodes, Electrochim. Acta 50 (2005) 4318–4326, http://dx.doi.org/10.1016/j.electacta.2005.02.093.

[51] G.E. Dima, A.C.A. De Vooys, M.T.M. Koper, Electrocatalytic reduction of nitrate at low concentration on coinage and transition-metal electrodes in acid solutions, J. Electroanal. Chem. 554–555 (2003) 15–23, http://dx.doi.org/10.1016/S0022-0728(02)01443-2.

[52] I. Katsounaros, G. Kyriacou, Influence of the concentration and the nature of the supporting electrolyte on the electrochemical reduction of nitrate on tin cathode, Electrochim. Acta 52 (2007) 6412–6420, http://dx.doi.org/10.1016/j.electacta.2007.04.050.

[53] K.D. Hristovski, J. Markovski, Engineering metal (hydr)oxide sorbents for removal of arsenate and similar weak-acid oxyanion contaminants: a critical review with emphasis on factors governing sorption processes, Sci. Total Environ. 598 (2017) 258–271, http://dx.doi.org/10.1016/j.scitotenv.2017.04.108.

[54] M.T. de Groot, M.T.M. Koper, The influence of nitrate concentration and acidity on the electrocatalytic reduction of nitrate on platinum, J. Electroanal. Chem. 562 (2004) 81–94, http://dx.doi.org/10.1016/j.jelechem.2003.08.011.

[55] C. Amatore, J.M. Saveant, Do ECE mechanisms occur in conditions where they could be characterized by electrochemical kinetic techniques? J. Electroanal. Chem. Interfacial Electrochem. 86 (1978) 227–232, http://dx.doi.org/10.1016/S0022-0728(78)80371-4.

[56] A.R. Cook, N. Dimitrijevic, B.W. Dreyfus, D. Meisel, L.A. Curtiss, D.M. Camaioni, Reducing radicals in nitrate solutions. The NO32- system revisited, J. Phys. Chem. A 105 (2001) 3658–3666, http://dx.doi.org/10.1021/jp0038052.

[57] H.O.N. Tugaoen, S. Garcia-Segura, K. Hristovski, P. Westerhoff, Challenges in photocatalytic reduction of nitrate as a water treatment technology, Sci. Total Environ. 599–600 (2017) 1524–1551, http://dx.doi.org/10.1016/j.scitotenv.2017.04.238.

[58] R. Tenne, K. Patel, K. Hashimoto, A. Fujishima, Efficient electrochemical reduction of nitrate to ammonia using conductive diamond film electrodes, J. Electroanal. Chem. 347 (1993) 409–415, http://dx.doi.org/10.1016/0022-0728(93)80105-Q.

[59] M. Fedurco, P. Kedzierzawski, J. Augustynski, Effect of multivalent cations upon reduction of nitrate ions at the Ag electrode, J. Electrochem. Soc. 146 (1999) 2569–2572, http://dx.doi.org/10.1149/1.1391973.

[60] V.N. Montesinos, N. Quici, H. Destaillats, M.I. Litter, Nitric oxide emission during the reductive heterogeneous photocatalysis of aqueous nitrate with TiO2, RSC Adv. 5 (2015) 85319–85322, http://dx.doi.org/10.1039/C5RA17914A.

[61] N.E. Khomutov, U.S. Stamkulov, Nitrate reduction at various metal electrodes, Sov. Electrochem. 7 (1971) 312–316.

[62] K.J. Vetter, Entgegnung auf die vorstehende Arbeit von G. Schmid iiber "Die autokatalytische Natur der kathodischen Reduktion von Salpetersaure zu salpetriger Saure", Z. Elektrochem. 63 (1959) 1189–1191.

[63] G. Schmid, Die autokatalytische Natur der kathodischen Reduktion von Salpetersäure zu salpetriger Säure I. Zur Deutung stationärer strom-Spannungs-Kurven, Z. Elektrochem. 63 (1959) 1183–1188, http://dx.doi.org/10.1002/bbpc.19590630927.

[64] G. Schmid, J. Delfs, Die autokatalytische Natur der kathodischen Reduktion von Salpetersäure zu salpetriger Säure II. Der galvanostatische Einschaltvorgang, Z. Elektrochem. 63 (1959) 1192–1197.

[65] G. Schmid, Die autokatalytische Natur der kathodischen Reduktion von Salpetersäure zu salpetriger Säure III. Mathematische Behandlung einer autokatalytischen Elektrodenreaktion 1. Ordnung, Z. Elektrochem. 65 (1961) 531–534.

[66] K.Y. Lee, D.J. Kuchynka, J.K. Kochi, Redox equilibria of the nitrosonium cation and of its nonbonded complexes, Inorg. Chem. 29 (1990) 4196–4204, http://dx.

doi.org/10.1021/ic00346a008.

[67] O.W.J.S. Rutten, A. Van Sandwijk, G. Van Weert, The electrochemical reduction of nitrate in acidic nitrate solutions, J. Appl. Electrochem. 29 (1999) 87–92, http://dx.doi.org/10.1023/A:1003412613806.

[68] M. Dortsiou, G. Kyriacou, Electrochemical reduction of nitrate on bismuth cathodes, J. Electroanal. Chem. 630 (2009) 69–74, http://dx.doi.org/10.1016/j.jelechem.2009.02.019.

[69] F. Balbaud, G. Sanchez, G. Santarini, G. Picard, Equilibria between gas and liquid phases for concentrated aqueous solutions of nitric acid, Eur. J. Inorg. Chem. 1999 (1999) 277–285, http://dx.doi.org/10.1002/(SICI)1099-0682(19990202)1999:2<277::AID-EJIC277>3.0.CO;2-#.

[70] V.P. Razygraev, M.V. Lebedeva, S.A. Kabakchi, Certain characteristics of the cathodic reduction of nitric acid on a platinum electrode, Dokl. Phys. Chem. 288 (1986) 1428–1432.

[71] J. Zheng, T. Lu, T.M. Cotton, G. Chumanov, Photoinduced electrochemical reduction of nitrite at an electrochemically roughened silver surface, J. Phys. Chem. B 103 (1999) 6567–6572, http://dx.doi.org/10.1021/jp990928h.

[72] S. Goldstein, D. Behar, T. Rajh, J. Rabani, Nitrite reduction to nitrous oxide and ammonia by TiO2 electrons in a colloid solution via consecutive one-electron transfer reactions, J. Phys. Chem. A 120 (2016) 2307–2312, http://dx.doi.org/10.1021/acs.jpca.6b01761.

[73] J.F. Su, I. Ruzybayev, I. Shah, C.P. Huang, The electrochemical reduction of nitrate over micro-architectured metal electrodes with stainless steel scaffold, Appl. Catal. B: Environ. 180 (2016) 199–209, http://dx.doi.org/10.1016/j.apcatb.2015.06.028.

[74] T. Yoshioka, K. Iwase, S. Nakanishi, K. Hashimoto, K. Kamiya, Electrocatalytic reduction of nitrate to nitrous oxide by a copper-modified covalent triazine framework, J. Phys. Chem. C 120 (2016) 15729–15734, http://dx.doi.org/10.1021/acs.jpcc.5b10962.

[75] I. Katsounaros, G. Kyriacou, Influence of nitrate concentration on its electrochemical reduction on tin cathode: identification of reaction intermediates, Electrochim. Acta 53 (2008) 5477–5484, http://dx.doi.org/10.1016/j.electacta.2008.03.018.

[76] A.C.A. De Vooys, G.L. Beltramo, B. Van Riet, J.A.R. Van Veen, M.T.M. Koper, Mechanisms of electrochemical reduction and oxidation of nitric oxide, Electrochim. Acta 49 (2004) 1307–1314, http://dx.doi.org/10.1016/j.electacta.2003.07.020.

[77] A.S. Dutton, J.M. Fukuto, K.N. Houk, Theoretical reduction potentials for nitrogen oxides from CBS-QB3 energetics and (C)PCM solvation calculations, Inorg. Chem. 44 (2005) 4024–4028, http://dx.doi.org/10.1021/ic048734q.

[78] D. De, J.D. Englehardt, E.E. Kalu, Electroreduction of nitrate and nitrite ion on a platinum-group-metal catalyst-modified carbon fiber electrode. Chronoamperometry and mechanism studies, J. Electrochem. Soc. 147 (2000) 4573–4579, http://dx.doi.org/10.1149/1.1394103.

[79] K. Tada, K. Shimazu, Kinetic studies of reduction of nitrate ions at Sn-modified Pt electrodes using a quartz crystal microbalance, J. Electroanal. Chem. 577 (2005) 303–309, http://dx.doi.org/10.1016/j.jelechem.2004.11.039.

[80] J. Yang, M. Duca, K.J.P. Schouten, M.T.M. Koper, Formation of volatile products during nitrate reduction on a Sn-modified Pt electrode in acid solution, J. Electroanal. Chem. 662 (2011) 87–92, http://dx.doi.org/10.1016/j.jelechem.2011.03.015.

[81] M. Duca, M.T.M. Koper, Powering denitrification: the perspectives of electrocatalytic nitrate reduction, Energy Environ. Sci. 5 (2012) 9726–9742, http://dx.doi.org/10.1039/c2ee23062c.

[82] R.F. Weiss, B.A. Price, Nitrous oxide solubility in water and seawater, Mar. Chem. 8 (1980) 347–359, http://dx.doi.org/10.1016/0304-4203(80)90024-9.

[83] M. Duca, M.O. Cucarella, P. Rodriguez, M.T.M. Koper, Direct reduction of nitrite to N2 on a Pt(100) electrode in alkaline media, J. Am. Chem. Soc. 132 (2010) 18042–18044, http://dx.doi.org/10.1021/ja1092503.

[84] M. Duca, M.C. Figueiredo, V. Climent, P. Rodriguez, J.M. Feliu, M.T.M. Koper, Selective catalytic reduction at quasi-perfect Pt (100) domains: a universal low-temperature pathway from nitrite to N2, J. Am. Chem. Soc. 133 (2011) 10928–10939.

[85] B. Kartal, J.G. Kuenen, M.C.M. van Loosdrecht, Sewage treatment with anammox, Science 328 (2010) 702–703, http://dx.doi.org/10.1126/science.1185941 (80-.).

[86] J.A. Harrison, R.G.A.R. Maclagan, A.R. Whyte, The structure and vibrational frequencies of NH2NO, Chem. Phys. Lett. 130 (1986) 98–102.

[87] D.A. Nguyen, M.A. Iwaniw, H.S. Fogler, Kinetics and mechanism of the reaction between ammonium and nitrite ions: experimental and theoretical studies, Chem. Eng. Sci. 58 (2003) 4351–4362, http://dx.doi.org/10.1016/S0009-2509(03)00317-8.

[88] I. Katsounaros, M. Dortsiou, C. Polatides, S. Preston, T. Kypraios, G. Kyriacou, Reaction pathways in the electrochemical reduction of nitrate on tin, Electrochim. Acta 71 (2012) 270–276, http://dx.doi.org/10.1016/j.electacta.2012.03.154.

[89] S.J. Klippenstein, L.B. Harding, P. Glarborg, Y. Gao, H. Hu, P. Marshall, Rate constant and branching fraction for the NH2 + NO2 reaction, J. Phys. Chem. A 117 (2013) 9011–9022, http://dx.doi.org/10.1021/jp4068069.

[90] P. Glarborg, K. Dam-Johansen, J.A. Miller, The reaction of ammonia with nitrogen dioxide in a flow reactor: implications for the NH2 + NO2 reaction, Int. J. Chem. Kinet. 27 (1995) 1207–1220, http://dx.doi.org/10.1002/kin.550271207.

[91] A.C.A. De Vooys, M.T.M. Koper, R.A. van Santen, J.A.R. van Veen, The role of adsorbates in the electrochemical oxidation of ammonia on noble and transition metal electrodes, J. Electroanal. Chem. 506 (2001) 127–137, http://dx.doi.org/10.1016/S0022-0728(01)00491-0.

[92] M.D. Bartberger, W. Liu, E. Ford, K.M. Miranda, C. Switzer, J.M. Fukuto, P.J. Farmer, D.A. Wink, K.N. Houk, The reduction potential of nitric oxide (NO) and its importance to NO biochemistry, Proc. Natl. Acad. Sci. U. S. A. 99 (2002) 10958–10963, http://dx.doi.org/10.1073/pnas.162095599.

[93] S. Wasmus, E.J. Vasini, M. Krausa, H.T. Mishima, W. Vielstich, DEMS-cyclic voltammetry investigation of the electrochemistry of nitrogen compounds in 0.5 M potassium hydroxide, Electrochim. Acta 39 (1994) 23–31, http://dx.doi.org/10.1016/0013-4686(94)85006-2.

[94] J.F.E. Gootzen, P.G.J.M. Peeters, J.M.B. Dukers, L. Lefferts, W. Visscher, J.A.R. van Veen, The electrocatalytic reduction of NO3− on Pt, Pd and Pt + Pd electrodes activated with Ge, J. Electroanal. Chem. 434 (1997) 171–183, http://dx.doi.org/10.1016/S0022-0728(97)00093-4.

[95] D. Reyter, D. Bélanger, L. Roué, Elaboration by high-energy ball milling of copper/palladium composite materials—characterization and electrocatalytic activity for the reduction of nitrate in alkaline medium, J. Electroanal. Chem. 622 (2008) 64–72, http://dx.doi.org/10.1016/j.jelechem.2008.05.002.

[96] E. Lacasa, P. Cañizares, J. Llanos, M.A. Rodrigo, Removal of nitrates by electrolysis in non-chloride media: effect of the anode material, Sep. Purif. Technol. 80 (2011) 592–599, http://dx.doi.org/10.1016/j.jhazmat.2012.02.034.

[97] H.O.N. Tugaoen, S. Garcia-Segura, K. Hristovski, P. Westerhoff, Compact light-emitting diode optical fiber immobilized TiO2 reactor for photocatalytic water treatment, Sci. Total Environ. 613–614 (2018) 1331–1338, http://dx.doi.org/10.1016/j.scitotenv.2017.09.242.

[98] J.R. Buchholz, R.E. Powell, The decomposition of hyponitrous acid. I. The Nonchain reaction, J. Am. Chem. Soc. 85 (1963) 509–511, http://dx.doi.org/10.1021/ja00888a004.

[99] G. Horányi, E.M. Rizmayer, Role of adsorption phenomena in the electrocatalytic reduction of nitric acid at a platinized platinum electrode, J. Electroanal. Chem. 140 (1982) 347–366, http://dx.doi.org/10.1016/0022-0728(82)85178-4.

[100] K. Nishimura, K. Machida, M. Enyo, On-line mass spectroscopy applied to electroreduction of nitrite and nitrate ions at porous Pt electrode in sulfuric acid solutions, Electrochim. Acta 36 (1991) 877–880, http://dx.doi.org/10.1016/0013-4686(91)85288-I.

[101] S. Taguchi, J.M. Feliu, Electrochemical reduction of nitrate on Pt(S)[n(111)×(111)] electrodes in perchloric acid solution, Electrochim. Acta 52 (2007) 6023–6033, http://dx.doi.org/10.1016/j.electacta.2007.03.057.

[102] S. Guo, K. Heck, S. Kasiraju, H. Qian, Z. Zhao, L.C. Grabow, J. Miller, M.S. Wong, Insights into nitrate reduction over indium-decorated palladium nanoparticle catalysts, ACS Catal. 8 (2018) 503–515, http://dx.doi.org/10.1021/acscatal.7b01371.

[103] B.P. Chaplin, M. Reinhard, W.F. Schneider, C. Schüth, J.R. Shapley, T.J. Strathmann, C.J. Werth, Critical review of Pd-based catalytic treatment of priority contaminants in water, Environ. Sci. Technol. 46 (2012) 3655–3670, http://dx.doi.org/10.1021/es204087q.

[104] P.M. Tucker, M.J. Waite, B.E. Hayden, Electrocatalytic reduction of nitrate on activated rhodium electrode surfaces, J. Appl. Electrochem. 34 (2004) 781–796, http://dx.doi.org/10.1023/B:JACH.0000035607.19248.b6.

[105] T. Ohmori, M.S. El-Deab, M. Osawa, Electroreduction of nitrate ion to nitrite and ammonia on a gold electrode in acidic and basic sodium and cesium nitrate solutions, J. Electroanal. Chem. 470 (1999) 46–52, http://dx.doi.org/10.1016/S0022-0728(99)00210-7.

[106] H. Kominami, A. Furusho, S. Murakami, H. Inoue, Effective photocatalytic reduction of nitrate to ammonia in an aqueous suspension of metal-loaded titanium (IV) oxide particles in the presence of oxalic acid, Catal. Lett. 76 (2001) 31–34, http://dx.doi.org/10.1023/A:1016771908609.

[107] O. Ghodbane, M. Sarrazin, L. Roué, D. Bélanger, Electrochemical reduction of nitrate on pyrolytic graphite-supported Cu and Pd–Cu electrocatalysts, J. Electrochem. Soc. 155 (2008) F117–F123, http://dx.doi.org/10.1149/1.2900094.

[108] O.A. Petrii, T.Y. Safonova, Electroreduction of nitrate and nitrite anions on platinum metals: a model process for elucidating the nature of the passivation by hydrogen adsorption, J. Electroanal. Chem. 331 (1992) 897–912, http://dx.doi.org/10.1016/0022-0728(92)85013-S.

[109] T.Y. Safonova, O.A. Petrii, Effect of inorganic cations on the electroreduction of nitrate anions on Pt/Pt electrodes in sulfuric acid solutions, J. Electroanal. Chem. 448 (1998) 211–216, http://dx.doi.org/10.1002/chin.199845027.

[110] C. Lu, S. Lu, W. Qiu, Q. Liu, Electroreduction of nitrate to ammonia in alkaline solutions using hydrogen storage alloy cathodes, Electrochim. Acta 44 (1999) 2193–2197.

[111] N. Barrabés, J. Just, A. Dafinov, F. Medina, J.L.G. Fierro, J.E. Sueiras, P. Salagre, Y. Cesteros, Catalytic reduction of nitrate on Pt-Cu and Pd-Cu on active carbon using continuous reactor: the effect of copper nanoparticles, Appl. Catal. B: Environ. 62 (2006) 77–85, http://dx.doi.org/10.1016/j.apcatb.2005.06.015.

[112] X. Huo, D.J. Van Hoomissen, J. Liu, S. Vyas, T.J. Strathmann, Hydrogenation of aqueous nitrate and nitrite with ruthenium catalysts, Appl. Catal. B: Environ. 211 (2017) 188–198, http://dx.doi.org/10.1016/j.apcatb.2017.04.045.

[113] O.A. Petrii, Y.A. Akbaeva, T.Y. Safonova, V.S. Kondrasheva, E.N. Kolosov, G.A. Tsirlina, V.M. Gryaznov, Intensification of the nitrate anion reduction on a membrane palladium electrode, Russ. J. Electrochem. 38 (2002) 220–223, http://dx.doi.org/10.1023/A:1016884718990.

[114] M. Li, C. Feng, Z. Zhang, Z. Shen, N. Sugiura, Electrochemical reduction of nitrate using various anodes and a Cu/Zn cathode, Electrochem. Commun. 11 (2009) 1853–1856, http://dx.doi.org/10.1016/j.elecom.2009.08.001.

[115] L. Wang, M. Li, X. Liu, C. Feng, F. Zhou, N. Chen, W. Hu, Mechanism and effectiveness of Ti-based nano-electrode for electrochemical denitrification, Int. J. Electrochem. Sci. 12 (2017) 1992–2002, http://dx.doi.org/10.20964/2017.03.50.

[116] M. Li, C. Feng, Z. Zhang, R. Chen, Q. Xue, C. Gao, N. Sugiura, Optimization of process parameters for electrochemical nitrate removal using Box-Behnken design, Electrochim. Acta 56 (2010) 265–270, http://dx.doi.org/10.1016/j.electacta.

2010.08.085.

[117] S. Garcia-Segura, J. Keller, E. Brillas, J. Radjenovic, Removal of organic contaminants from secondary effluent by anodic oxidation with a boron-doped diamond anode as tertiary treatment, J. Hazard. Mater. 283 (2015) 551–557, http://dx.doi.org/10.1016/j.jhazmat.2014.10.003.

[118] M. Deborde, U. von Gunten, Reactions of chlorine with inorganic and organic compounds during water treatment-kinetics and mechanisms: a critical review, Water Res. 42 (2008) 13–51, http://dx.doi.org/10.1016/j.watres.2007.07.025.

[119] J. Llanos, S. Cotillas, P. Cañizares, M.A. Rodrigo, Novel electrodialysis-electrochlorination integrated process for the reclamation of treated wastewaters, Sep. Purif. Technol. 132 (2014) 362–369, http://dx.doi.org/10.1016/j.seppur.2014.05.017.

[120] J.S. Nicoson, D.W. Margerum, Kinetics and mechanisms of aqueous chlorine reactions with chlorite ion in the presence of chloride ion and acetic acid/acetate buffer, Inorg. Chem. 41 (2002) 342–347, http://dx.doi.org/10.1021/ic010762a.

[121] B.M. Saunier, R.E. Selleck, The kinetics of breakpoint chlorination in continuous flow systems, J. Am. Water Work Assoc. 71 (1979) 164–172.

[122] X. Zhang, W. Li, E.R. Blatchley, X. Wang, P. Ren, UV/chlorine process for ammonia removal and disinfection by-product reduction: comparison with chlorination, Water Res. 68 (2015) 804–811, http://dx.doi.org/10.1016/j.watres.2014.10.044.

[123] G. Hua, D.A. Reckhow, Comparison of disinfection byproduct formation from chlorine and alternative disinfectants, Water Res. 41 (2007) 1667–1678, http://dx.doi.org/10.1016/j.watres.2007.01.032.

[124] C.M.M. Bougeard, E.H. Goslan, B. Jefferson, S.A. Parsons, Comparison of the disinfection by-product formation potential of treated waters exposed to chlorine and monochloramine, Water Res. 44 (2010) 729–740, http://dx.doi.org/10.1016/j.watres.2009.10.008.

[125] X. Ma, M. Li, C. Feng, W. Hu, L. Wang, X. Liu, Development and reaction mechanism of efficient nano titanium electrode: reconstructed nanostructure and enhanced nitrate removal efficiency, J. Electroanal. Chem. 782 (2016) 270–277, http://dx.doi.org/10.1016/j.jelechem.2016.10.047.

[126] W. Lee, P. Westerhoff, Formation of organic chloramines during water disinfection– chlorination versus chloramination, Water Res. 43 (2009) 2233–2239, http://dx.doi.org/10.1016/j.watres.2009.02.009.

[127] D.G. Neden, R.J. Jones, J.R. Smith, G.J. Kirmeyer, G.W. Foust, Chlorination and chloramination for controlling bacterial regrowth, J. Am. Water Work Assoc. 84 (1992) 80–88.

[128] D.L. Sedlak, U. von Gunten, The chlorine dilemma, Science 331 (2011) 42–43 (80-.).

[129] J.C. Crittenden, R.R. Trussel, D.W. Hand, K.J. Howe, G. Tchobanoglous, Water Treatment Principles and Design, 3rd ed., Wiley, New Jersey, 2012.

[130] M. Li, C. Feng, Z. Zhang, N. Sugiura, Efficient electrochemical reduction of nitrate to nitrogen using Ti/IrO2-Pt anode and different cathodes, Electrochim. Acta 54 (2009) 4600–4606, http://dx.doi.org/10.1016/j.electacta.2009.03.064.

[131] D. Reyter, D. Bélanger, L. Roué, Nitrate removal by a paired electrolysis on copper and Ti/IrO2 coupled electrodes – influence of the anode/cathode surface area ratio, Water Res. 44 (2010) 1918–1926, http://dx.doi.org/10.1016/j.watres.2009.11.037.

[132] F. Liu, M. Li, H. Wang, X. Lei, L. Wang, X. Liu, Fabrication and characterization of a Cu-Zn-TiO2 nanotube array polymetallic nanoelectrode for electrochemically removing nitrate from groundwater, J. Electrochem. Soc. 163 (2016) E421–E427, http://dx.doi.org/10.1149/2.1391614jes.

[133] W. Teng, N. Bai, Y. Liu, Y. Liu, J. Fan, W. Zhang, Selective nitrate reduction to dinitrogen by electrocatalysis on nanoscale iron encapsulated in mesoporous carbon, Environ. Sci. Technol. 52 (2018) 230–236, http://dx.doi.org/10.1021/acs.est.7b04775.

[134] I.G. Casella, M. Ritorti, Electrodeposition of silver particles from alkaline aqueous solutions and their electrocatalytic activity for the reduction of nitrate, bromate and chlorite ions, Electrochim. Acta 55 (2010) 6462–6468, http://dx.doi.org/10.1016/j.electacta.2010.06.038.

[135] D. Reyter, D. Bélanger, L. Roué, Optimization of the cathode material for nitrate removal by a paired electrolysis process, J. Hazard. Mater. 192 (2011) 507–513, http://dx.doi.org/10.1016/j.jhazmat.2011.05.054.

[136] D. Reyter, M. Odziemkowski, D. Bélanger, L. Roué, Electrochemically activated copper electrodes, J. Electrochem. Soc. 154 (2007) K36–K44, http://dx.doi.org/10.1149/1.2746805.

[137] N. Aouina, H. Cachet, C. Debiemme-Chouvy, T.T.M. Tran, Insight into the electroreduction of nitrate ions at a copper electrode, in neutral solution, after determination of their diffusion coefficient by electrochemical impedance spectroscopy, Electrochim. Acta 55 (2010) 7341–7345, http://dx.doi.org/10.1016/j.electacta.2010.07.032.

[138] K. Bouzek, M. Paidar, A. Sadílková, H. Bergmann, Electrochemical reduction of nitrate in weakly alkaline solutions, J. Appl. Electrochem. 31 (2001) 1185–1193, http://dx.doi.org/10.1023/A:1012755222981.

[139] O.G. Pérez, J.M. Bisang, Removal of nitrate using an activated rotating cylinder electrode, Electrochim. Acta 194 (2016) 448–453, http://dx.doi.org/10.1016/j.electacta.2016.02.114.

[140] A.S. Lima, M.O. Salles, T.L. Ferreira, T.R.L.C. Paixão, M. Bertotti, Scanning electrochemical microscopy investigation of nitrate reduction at activated copper cathodes in acidic medium, Electrochim. Acta 78 (2012) 446–451, http://dx.doi.org/10.1016/j.electacta.2012.06.075.

[141] K.S. Rajmohan, C. Raghuram, Nitrate reduction at electrodeposited copper on copper cathode, ECS Trans. 59 (2014) 397–411.

[142] I.G. Zacharia, W.M. Deen, Diffusivity and solubility of nitric oxide in water and saline, Ann. Biomed. Eng. 33 (2005) 214–222, http://dx.doi.org/10.1007/s10439-005-8980-9.

[143] M. Nobial, O. Devos, O.R. Mattos, B. Tribollet, The nitrate reduction process: a way for increasing interfacial pH, J. Electroanal. Chem. 600 (2007) 87–94, http://dx.doi.org/10.1016/j.jelechem.2006.03.003.

[144] M.S. El-Deab, Electrochemical reduction of nitrate to ammonia at modified gold electrodes, Electrochim. Acta 49 (2004) 1639–1645, http://dx.doi.org/10.1016/j.electacta.2003.11.025.

[145] F.R. Hartley, Chemistry of the Platinum Group Metals—Recent Developments, Elsevier, New York, 1991, http://dx.doi.org/10.1016/B978-0-444-88189-2.50012-2.

[146] P.B. Kettler, Platinum group metals in catalysis: fabrication of catalysts and catalyst precursors, Org. Process Res. Dev. 7 (2003) 342–354, http://dx.doi.org/10.1021/op034017o.

[147] B.S. Khangarot, S. Das, Acute toxicity of metals and reference toxicants to a freshwater ostracod, Cypris subglobosa Sowerby, 1840 and correlation to EC50 values of other test models, J. Hazard. Mater. 172 (2009) 641–649, http://dx.doi.org/10.1016/j.jhazmat.2009.07.038.

[148] M.C.P.M. da Cunha, J.P.I. de Souza, F.C. Nart, Reaction pathways for reduction of nitrate ions on platinum, rhodium, and platinum-rhodium alloy electrodes, Langmuir 16 (2000) 771–777, http://dx.doi.org/10.1021/la990638s.

[149] S. Ureta-Zañartu, C. Yáñez, Electroreduction of nitrate ion on Pt, Ir and on 70:30 Pt:Ir alloy, Electrochim. Acta 42 (1997) 1725–1731, http://dx.doi.org/10.1016/S0013-4686(96)00372-6.

[150] B. Hammer, J.K. Norskov, Theoretical surface science and catalysis—calculations and concepts, Adv. Catal. 45 (2000) 71–129, http://dx.doi.org/10.1016/S0360-0564(02)45013-4.

[151] F. Calle-Vallejo, M. Huang, J.B. Henry, M.T.M. Koper, A.S. Bandarenka, Theoretical design and experimental implementation of Ag/Au electrodes for the electrochemical reduction of nitrate, Phys. Chem. Chem. Phys. 15 (2013) 3196–3202, http://dx.doi.org/10.1039/c2cp44620k.

[152] M. Li, C. Feng, Z. Zhang, S. Yang, N. Sugiura, Treatment of nitrate contaminated water using an electrochemical method, Bioresour. Technol. 101 (2010) 6553–6557, http://dx.doi.org/10.1016/j.biortech.2010.03.076.

[153] P. Kuang, C. Feng, N. Chen, W. Hu, G. Wang, T. Peng, L. Lv, Improvement on electrochemical nitrate removal by combining with the three-dimensional (3-D) perforated iron cathode and the iron net introduction, J. Electrochem. Soc. 163 (2016) E397–E406, http://dx.doi.org/10.1149/2.0881614jes.

[154] H. Duarte, K. Jha, J. Weidner, Electrochemical reduction of nitrates and nitrites in alkaline media in the presence of hexavalent chromium, J. Appl. Electrochem. 28 (1998) 811–817, http://dx.doi.org/10.1023/A:1003459603696.

[155] L. Durivault, O. Brylev, D. Reyter, M. Sarrazin, D. Bélanger, L. Roué, Cu-Ni materials prepared by mechanical milling: their properties and electrocatalytic activity towards nitrate reduction in alkaline medium, J. Alloys Compd. 432 (2007) 323–332, http://dx.doi.org/10.1016/j.jallcom.2006.06.023.

[156] I. Katsounaros, D. Ipsakis, C. Polatides, G. Kyriacou, Efficient electrochemical reduction of nitrate to nitrogen on tin cathode at very high cathodic potentials, Electrochim. Acta 52 (2006) 1329–1338, http://dx.doi.org/10.1016/j.electacta.2006.07.034.

[157] WHO, Inorganic Tin in Drinking-Water Background Document for Development of WHO, Guidelines for Drinking-water Quality, 2004, http://www.who.int/water_sanitation_health/dwq/chemicals/tin.pdf.

[158] B. Ambrosioni, A. Barthelemy, D. Bejan, N.J. Bunce, Electrochemical reduction of aqueous nitrate ion at tin cathodes, Can. J. Chem. 92 (2014) 228–233, http://dx.doi.org/10.1139/cjc-2013-0406.

[159] M. Dortsiou, I. Katsounaros, C. Polatides, G. Kyriacou, Electrochemical removal of nitrate from the spent regenerant solution of the ion exchange, Desalination 248 (2009) 923–930, http://dx.doi.org/10.1016/j.desal.2008.10.012.

[160] J. Kearns, A. Turner, An evaluation of the toxicity and bioaccumulation of bismuth in the coastal environment using three species of macroalga, Environ. Pollut. 208 (2016) 435–441, http://dx.doi.org/10.1016/j.envpol.2015.10.011.

[161] A. Atwal, G.C.S. Cousin, Bismuth toxicity in patients treated with bismuth iodoform paraffin packs, Br. J. Oral Maxillofac. Surg. 54 (2016) 111–112, http://dx.doi.org/10.1016/j.bjoms.2015.09.009.

[162] C. Polatides, M. Dortsiou, G. Kyriacou, Electrochemical removal of nitrate ion from aqueous solution by pulsing potential electrolysis, Electrochim. Acta 50 (2005) 5237–5241, http://dx.doi.org/10.1016/j.electacta.2005.01.057.

[163] A.M. Shams El Din, F.M. Abd El Wahab, The behaviour of copper-zinc alloys in alkaline solutions upon alternate anodic and cathodic polarization, Electrochim. Acta 10 (1965) 1127–1140, http://dx.doi.org/10.1016/0010-938X(77)90039-7.

[164] Z. Mácová, K. Bouzek, Electrocatalytic activity of copper alloys for NO3- reduction in a weakly alkaline solution part 1: copper-zinc, J. Appl. Electrochem. 35 (2005) 1203–1211, http://dx.doi.org/10.1007/s10800-005-9028-4.

[165] L. Mattarozzi, S. Cattarin, N. Comisso, R. Gerbasi, P. Guerriero, M. Musiani, L. Vazquez-Gomez, E. Verlato, Electrodeposition of compact and porous Cu-Zn alloy electrodes and their use in the cathodic reduction of nitrate, J. Electrochem. Soc. 162 (2015) D236–D241, http://dx.doi.org/10.1149/2.1041506jes.

[166] M. Li, C. Feng, Z. Zhang, X. Lei, R. Chen, Y. Yang, N. Sugiura, Simultaneous reduction of nitrate and oxidation of by-products using electrochemical method, J. Hazard. Mater. 171 (2009) 724–730, http://dx.doi.org/10.1016/j.jhazmat.2009.06.066.

[167] N. Fan, Z. Li, L. Zhao, N. Wu, T. Zhou, Electrochemical denitrification and kinetics study using Ti/IrO2-TiO2-RuO2 as the anode and Cu/Zn as the cathode, Chem. Eng. J. 214 (2013) 83–90, http://dx.doi.org/10.1016/j.cej.2012.10.026.

[168] USEPA, Secondary Drinking Water Standards: Guidance for Nuisance Chemicals On This Page: What Are Secondary Standards? Why Set Secondary Standards? What Problems Are Caused by These Contaminants? (2017), pp. 1–6 https://www.epa.gov/dwstandardsregulations/secondary-drinking-water-standards-guidance-

nuisance-chemicals.

[169] WHO, Zinc in Drinking-Water, (2003), http://dx.doi.org/10.1038/ki.2011.410.

[170] L. Mattarozzi, S. Cattarin, N. Comisso, P. Guerriero, M. Musiani, L. Vázquez-Gómez, E. Verlato, Electrochemical reduction of nitrate and nitrite in alkaline media at CuNi alloy electrodes, Electrochim. Acta 89 (2013) 488–496, http://dx.doi.org/10.1016/j.electacta.2012.11.074.

[171] T. Chen, H. Li, H. Ma, M.T.M. Koper, Surface modification of Pt(100) for electrocatalytic nitrate reduction to dinitrogen in alkaline solution, Langmuir 31 (2015) 3277–3281, http://dx.doi.org/10.1021/acs.langmuir.5b00283.

[172] S. Amertharaj, M.A. Hasnat, N. Mohamed, Electroreduction of nitrate ions at a platinum-copper electrode in an alkaline medium: influence of sodium inositol phytate, Electrochim. Acta 136 (2014) 557–564, http://dx.doi.org/10.1016/j.electacta.2014.05.128.

[173] A.C.A. de Vooys, R.A. van Santen, J.A.R. van Veen, Electrocatalytic reduction of NO y on palladiumrcopper 3 electrodes, J. Mol. Catal. A: Chem. 154 (2000) 203–215, http://dx.doi.org/10.1016/S1381-1169(99)00375-1.

[174] D. Reyter, D. Bélanger, L. Roué, Elaboration of Cu-Pd films by coelectrodeposition: application to nitrate electroreduction, J. Phys. Chem. C 113 (2009) 290–297, http://dx.doi.org/10.1021/jp805484t.

[175] K.-W. Kim, S.-M. Kim, Y.-H. Kim, E.-H. Lee, K.-Y. Jee, Sn stability of Sn-modified Pt electrode for reduction of nitrate, J. Electrochem. Soc. 154 (2007) E145–E152, http://dx.doi.org/10.1149/1.2769286.

[176] Y. Wang, Y. Rao, The electrocatalytic reduction of nitrate in water on Pd/Sn-modified actiated carbon fier electrode, Water Res. 40 (2006) 1224–1236, http://dx.doi.org/10.1016/j.watres.2006.01.017.

[177] K. Shimazu, R. Goto, S. Piao, R. Kayama, K. Nakata, Y. Yoshinaga, Reduction of nitrate ions on tin-modified palladium thin film electrodes, J. Electroanal. Chem. 601 (2007) 161–168, http://dx.doi.org/10.1016/j.jelechem.2006.11.005.

[178] K. Tada, T. Kawaguchi, K. Shimazu, High electrocatalytic performance of Pd/Sn/Au electrodes for nitrate reduction, J. Electroanal. Chem. 572 (2004) 93–99, http://dx.doi.org/10.1016/j.jelechem.2004.06.004.

[179] I.G. Casella, M. Contursi, An electrochemical and XPS study of the electrodeposited binary Pd-Sn catalyst: the electroreduction of nitrate ions in acid medium, J. Electroanal. Chem. 588 (2006) 147–154, http://dx.doi.org/10.1016/j.jelechem.2005.12.015.

[180] M. Motahar Hossain, K. Nakata, T. Kawaguchi, K. Shimazu, Reduction of nitrate on electrochemically pre-reduced tin-modified palladium electrodes, J. Electroanal. Chem. 707 (2013) 59–65, http://dx.doi.org/10.1016/j.jelechem.2013.08.015.

[181] Y. Einaga, J.S. Foord, G.M. Swain, Diamond electrodes: diversity and maturity, Mater. Res. Bull. 39 (2014) 525–532, http://dx.doi.org/10.1557/mrs.2014.94.

[182] S. Garcia-Segura, E. Vieira dos Santos, C.A. Martínez-Huitle, Role of sp3/sp2 ratio on the electrocatalytic properties of boron-doped diamond electrodes: a mini review, Electrochem. Commun. 59 (2015) 52–55, http://dx.doi.org/10.1016/j.elecom.2015.07.002.

[183] R. Dewil, D. Mantzavinos, I. Poulios, M.A. Rodrigo, New perspectives for advanced oxidation processes, J. Environ. Manage. 195 (2017) 93–99, http://dx.doi.org/10.1016/j.jenvman.2017.04.010.

[184] F. Bouamrane, A. Tadjeddine, J.E. Butler, R. Tenne, C. Lévy-Clément, Electrochemical study of diamond thin films in neutral and basic solutions of nitrate, J. Electroanal. Chem. 405 (1996) 95–99, http://dx.doi.org/10.1016/0022-0728(95)04388-8.

[185] C. Reuben, E. Galun, H. Cohen, R. Tenne, R. Kalish, Y. Muraki, K. Hashimoto, A. Fujishima, J.M. Butler, C. Lévy-Clément, Efficient reduction of nitrite and nitrate to ammonia using thin-film B-doped diamond electrodes, J. Electroanal. Chem. 396 (1995) 233–239, http://dx.doi.org/10.1016/0022-0728(95)03961-F.

[186] A.N. Ndao, F. Zenia, A. Deneuville, M. Bernard, C. Lévy-Clément, Effect of boron concentration on the electrochemical reduction of nitrates on polycrystalline diamond electrodes, Diam. Relat. Mater. 9 (2000) 1175–1180, http://dx.doi.org/10.1016/S0925-9635(99)00328-3.

[187] C. Lévy-Clément, N.A. Ndao, A. Katty, M. Bernard, A. Deneuville, C. Comninellis, A. Fujishima, Boron doped diamond electrodes for nitrate elimination in concentrated wastewater, Diam. Relat. Mater. 12 (2003) 606–612, http://dx.doi.org/10.1016/S0925-9635(02)00368-0.

[188] J.T. Matsushima, A.F. Azevedo, M.R. Baldan, N.G. Ferreira, The grain size influence on boron doped diamond sensitivity for nitrate electrochemical reduction, ECS Trans. 25 (2010) 53–58.

[189] D.A. Tryk, K. Tsunozaki, T.N. Rao, A. Fujishima, Relationships between surface character and electrochemical processes on diamond electrodes: dual roles of surface termination and near-surface hydrogen, Diam. Relat. Mater. 10 (2001) 1804–1809, http://dx.doi.org/10.1016/S0925-9635(01)00453-8.

[190] M.C. Granger, M. Witek, J. Xu, J. Wang, M. Hupert, A. Hanks, M.D. Koppang, J.E. Butler, G. Lucazeau, M. Mermoux, J.W. Strojek, G.M. Swain, Standard electrochemical behavior of high-quality, boron-doped polycrystalline diamond thin-film electrodes, Anal. Chem. 72 (2000) 3793–3804, http://dx.doi.org/10.1021/ac0000675.

[191] D. Medeiros De Araújo, P. Cañizares, C.A. Martínez-Huitle, M.A. Rodrigo, Electrochemical conversion/combustion of a model organic pollutant on BDD anode: role of sp3/sp2 ratio, Electrochem. Commun. 47 (2014) 37–40, http://dx.doi.org/10.1016/j.elecom.2014.07.017.

[192] F.L. Souza, C. Sáez, M.R.V. Lanza, P. Cañizares, M.A. Rodrigo, Electrochimica acta the effect of the sp3/sp2 carbon ratio on the electrochemical oxidation of 2,4-D with p-Si BDD anodes, Electrochim. Acta 187 (2016) 119–124.

[193] T. Watanabe, Y. Honda, K. Kanda, Y. Einaga, Tailored design of boron-doped diamond electrodes for various electrochemical applications with boron-doping level and sp2-bonded carbon impurities, Phys. Status Solidi Appl. Mater. Sci. 211

(2014) 2709–2717, http://dx.doi.org/10.1002/pssa.201431455.

[194] J.A. Epstein, I. Levin, S. Raviv, Electrochemical reduction of dilute nitric acid, Electrochim. Acta 9 (1964) 1665–1673, http://dx.doi.org/10.1016/0013-4686(64)80093-1.

[195] O. Brylev, M. Sarrazin, D. Bélanger, L. Roué, Rhodium deposits on pyrolytic graphite substrate: physico-chemical properties and electrocatalytic activity towards nitrate reduction in neutral medium, Appl. Catal. B: Environ. 64 (2006) 243–253, http://dx.doi.org/10.1016/j.apcatb.2005.11.016.

[196] O. Brylev, M. Sarrazin, L. Roué, D. Bélanger, Nitrate and nitrite electrocatalytic reduction on Rh-modified pyrolytic graphite electrodes, Electrochim. Acta 52 (2007) 6237–6247, http://dx.doi.org/10.1016/j.electacta.2007.03.072.

[197] L.A. Estudillo-Wong, N. Alonso-Vante, A. Manzo-Robledo, Electro-reduction of nitrate and nitrite ions on carbon-supported Pt nanoparticles, ECS Trans. 15 (2008) 385–393, http://dx.doi.org/10.1149/1.3046654.

[198] L.A. Estudillo-Wong, E.M. Arce-Estrada, N. Alonso-Vante, A. Manzo-Robledo, Electro-reduction of nitrate species on Pt-based nanoparticles: surface area effects, Catal. Today 166 (2011) 201–204, http://dx.doi.org/10.1016/j.cattod.2010.09.010.

[199] S.N. Pronkin, P.A. Simonov, V.I. Zaikovskii, E.R. Savinova, Model Pd-based bimetallic supported catalysts for nitrate electroreduction, J. Mol. Catal. A: Chem. 265 (2007) 141–147, http://dx.doi.org/10.1016/j.molcata.2006.10.007.

[200] J.W. Peel, K.J. Reddy, B.P. Sullivan, J.M. Bowen, Electrocatalytic reduction of nitrate in water, Water Res. 37 (2003) 2512–2519, http://dx.doi.org/10.1016/S0043-1354(03)00008-3.

[201] D. Pan, W. Lu, S. Wu, H. Zhang, W. Qin, In situ spontaneous redox synthesis of carbon nanotubes/copper oxide nanocomposites and their preliminary application in electrocatalytic reduction of nitrate, Mater. Lett. 89 (2012) 333–335, http://dx.doi.org/10.1016/j.matlet.2012.09.004.

[202] I.G. Casella, M. Gatta, Electrochemical reduction of NO3- and NO 2- on a composite copper thallium electrode in alkaline solutions, J. Electroanal. Chem. 568 (2004) 183–188, http://dx.doi.org/10.1016/j.jelechem.2004.01.021.

[203] T. Öznülüer, B. Özdurak, H.Ö. Doğan, Electrochemical reduction of nitrate on graphene modified copper electrodes in alkaline media, J. Electroanal. Chem. 699 (2013) 1–5, http://dx.doi.org/10.1016/j.jelechem.2013.04.001.

[204] P. Westerhoff, P. Alvarez, Q. Li, J. Gardea-Torresdey, J. Zimmerman, Overcoming implementation barriers for nanotechnology in drinking water treatment, Environ. Sci. Nano 3 (2016) 1241–1253, http://dx.doi.org/10.1039/C5EN00253B.

[205] E.B. Molodkina, I.G. Botryakova, A.I. Danilov, J. Souza-Garcia, J.M. Feliu, Mechanism of nitrate electroreduction on Pt(100), Russ. J. Electrochem. 48 (2012) 302–315, http://dx.doi.org/10.1134/S1023193512020115.

[206] S.-E. Bae, A.A. Gewirth, Differential reactivity of Cu(111) and Cu(100) during nitrate reduction in acid electrolyte, Faraday Discuss. 140 (2009) 113–123, http://dx.doi.org/10.1039/B814058H.

[207] A.P. Leontiev, O.A. Brylev, K.S. Napolskii, Arrays of rhodium nanowires based on anodic alumina: preparation and electrocatalytic activity for nitrate reduction, Electrochim. Acta 155 (2015) 466–473, http://dx.doi.org/10.1016/j.electacta.2014.12.073.

[208] K. Jha, J.W. Weidner, Evaluation of porous cathodes for the electrochemical reduction of nitrates and nitrites in alkaline waste streams, J. Appl. Electrochem. 29 (1999) 1305–1315, http://dx.doi.org/10.1023/A:1003753220647.

[209] M. Gifford, M. Chester, K. Hristovski, P. Westerhoff, Human health tradeoffs in wellhead drinking water treatment: comparing exposure reduction to embedded life cycle risks, Water Res. 128 (2018) 246–254, http://dx.doi.org/10.1016/j.carbon.2017.06.039.

[210] G. Sposito, The Environmental Chemistry of Aluminum, 2nd ed., Lewis Publishers, New York, 1996.

[211] E.E. Ferapontova, N.V. Fedorovich, Effect of cation adsorption on the kinetics of anion electroreduction part I. Effect of the adsorption of inorganic cations in small concentrations on the kinetics of anion electroreduction with different elementary steps of discharge, J. Electroanal. Chem. 476 (1999) 26–36, http://dx.doi.org/10.1016/S0022-0728(99)00360-5.

[212] L. Ma, B.-Y. Zhang, H.-L. Li, J.Q. Chambers, Kinetics of nitrate reduction by cobalt-cyclam incorporated Nafion redox polymer, J. Electroanal. Chem. 362 (1993) 201–205, http://dx.doi.org/10.1016/0022-0728(93)80022-A.

[213] J. Shen, Y.Y. Birdja, M.T.M. Koper, Electrocatalytic nitrate reduction by a cobalt protoporphyrin immobilized on a pyrolytic graphite electrode, Langmuir 31 (2015) 8495–8501, http://dx.doi.org/10.1021/acs.langmuir.5b00977.

[214] Y.Y. Birdja, J. Yang, M.T.M. Koper, Electrocatalytic reduction of nitrate on tin-modified palladium electrodes, Electrochim. Acta 140 (2014) 518–524, http://dx.doi.org/10.1016/j.electacta.2014.06.011.

[215] M.C.E. Ribeiro, A.B. Couto, N.G. Ferreira, M.R. Baldan, NoNitrate removal by electrolysis using Cu/BDD electrode cathode, ECS Trans. 58 (2014) 21–26.

[216] X. Xing, D.A. Scherson, The electrocatalytic reduction of nitrate mediated by underpotential-deposited cadmium on gold and silver electrodes in acid media, J. Electrochem. Soc. 137 (1990) 2166–2175.

[217] T.T.P. Nguyen, B.K.D. Do, N.N. Bui, M.A. Pham, T.V. Nguyen, Selectiveness of copper and polypyrrole modified copper electrodes for nitrate electroreduction: a comparative study and application in ground water, ECS Trans. 53 (2013) 41–52, http://dx.doi.org/10.1149/05316.0041ecst.

[218] Dmarcus100, Periodic Table Of Elements Black And White SVG. [CC BY-SA 4.0, (2016) https://creativecommons.org/licenses/by-sa/4.0)].

[219] L. Mattarozzi, S. Cattarin, N. Comisso, R. Gerbasi, P. Guerriero, M. Musiani, L. Vazquez-Gomez, E. Verlato, Electrodeposition of Cu-Ni alloy electrodes with bimodal porosity and their use for nitrate reduction, ECS Electrochem. Lett. 2 (2013) D58–D60, http://dx.doi.org/10.1149/2.004311eel.